Aus der Klinik und Poliklinik für Neurologie
der Universitätsmedizin der Johannes Gutenberg-Universität Mainz

CENTRAL NERVOUS SYSTEM-INTRINSIC DETERMINANTS OF T-CELL-INDUCED NEUROINFLAMMATION

DIE ROLLE ZNS-INTRINSISCHER EINFLUSSFAKTOREN FÜR DIE T-ZELL-INDUZIERTE NEUROINFLAMMATION

Inauguraldissertation
Zur Erlangung des Doktorgrades der
Medizin
der Universitätsmedizin
der Johannes Gutenberg-Universität Mainz

Vorgelegt von

Julia Loos
aus Worms

Mainz, 2020

Wissenschaftlicher Vorstand:

1. Gutachter:

2. Gutachter:

Tag der Promotion: 06.07.2021

PUBLICATION LIST

The doctoral thesis is based on following own publications

(1) *Functional characteristics of Th1, Th17 and ex-Th17-cells in EAE revealed by intravital two-photon microscopy*
Julia Loos*, Samantha Schmaul*, Theresa Noll, Magdalena Paterka, Miriam Schillner, Julian Löffel, Frauke Zipp and Stefan Bittner

J Neuroinflammation, accepted for publication
*equally contributing

(2) *MOG Encephalomyelitis: Distinct Clinical, MRI and CSF Features in Patients With Longitudinal Extensive Transverse Myelitis as First Clinical Presentation*
Julia Loos, Steffen Pfeuffer, Katrin Pape, Tobias Ruck, Felix Luessi, Annette Spreer, Frauke Zipp, Sven G Meuth and Stefan Bittner

J Neurol. 2020 Jun;267(6):1632-1642. doi: 10.1007/s00415-020-09755-x. Epub 2020 Feb 13.

(3) *Neuronal ICAM-5 Plays a Neuroprotective Role in Progressive Neurodegeneration*
Katharina Birkner*, **Julia Loos***, René Gollan, Falk Steffen, Beatrice Wasser, Tobias Ruck, Sven G. Meuth, Frauke Zipp and Stefan Bittner

Front Neurol. 2019 Mar 12;10:205. doi: 10.3389/fneur.2019.00205. eCollection 2019. *equally contributing

(4) *The Role of ERK Signaling in Experimental Autoimmune Encephalomyelitis*
Katharina Birkner, Beatrice Wasser, **Julia Loos**, Alexander Plotnikov, Rony Seger, Frauke Zipp, Esther Witsch and Stefan Bittner

Int J Mol Sci. 2017 Sep 15; 18(9):1990. doi: 10.3390/ijms18091990.

TABLE OF CONTENTS

LIST OF ABBREVIATIONS

°C	degree Celsius
3D	three dimensional
AHR	aryl hydrocarbon receptor
APC	antigen presenting cell
BBB	blood-brain barrier
BME	basal medium eagle
BSA	albumin bovine
CD	cluster of differentiation
cDNA	complementary DNA
CFA	complete Freund's adjuvant
CFP	cyan fluorescent protein
CFSE	carboxyfluorescein succinimidyl ester
CIS	clinically isolated syndrome
CNS	central nervous system
CO_2	carbon dioxide
CSF	cerebrospinal fluid
d	day
DAPI	4',6-Diamidino-2-phenylindole dihydrochloride
DIV	days in vitro
DMEM	Dulbecco's modified eagle medium
DMSO	dimethyl sulfoxide
DMT	disease modifying therapy
EAE	experimental autoimmune encephalomyelitis
EDSS	expanded disability status scale
EDTA	ethylenediaminetetraacetic acid
ELISA	enzyme-linked immunosorbent assay

EtOH	ethanol
FBS	fetal bovine serum
FITC	fluorescein isothiocyanate
FoxP3	forkhead box P3
G	gauge
g	gram
GFP	green fluorescence protein
Gy	gray
h	hours
HBSS	Hank's balanced salt solution
HEPES	4-(2-hydroxyethyl)-1-piperazineethanesulfonic acid
HIHS	heat inactivated horse serum
ICAM	intercellular adhesion molecule
IFN	interferon
Ig	immunoglobulin
IL	interleukin
IPEX	immune dysregulation, polyendocrinopathy, enteropathy and X-linked inheritance
kg	kilogram
KO	knockout
LFA	lymphocyte function-associated antigen
LPS	lipopolysaccharide
MAP	microtubule-associated protein
MBP	myelin basic protein
MEM	minimum essential medium
mg	milligram
$MgCl_2$	magnesium chloride

MHC	major histocompatibility complex
min	minutes
ml	milliliter
MMP	matrix metalloproteinase
MOG	myelin oligodendrocyte glycoprotein
mRNA	messenger RNA
MS	multiple sclerosis
NaCl	sodium chloride
NEDA	no evidence of disease activity
NH_4Cl	ammonium chloride
NIND	non-inflammatory neurological disease
nm	nanometers
ns	not significant
OPO	optical parametric oscillator
P	postnatally
p	probability
P/S	penicillin/streptomycin
PB	phosphate buffer
PBS	Dulbecco's phosphate-buffered saline
PCR	polymerase chain reaction
PFA	paraformaldehyde
pH	potential of hydrogen
PI	propidium iodide
PNS	peripheral nerve system
PPMS	primary-progressive multiple sclerosis
PTX	pertussis toxin
Rag	recombinant activating gene

RFP	red fluorescent protein
RORγ	RAR related orphan receptor gamma
RRMS	relapsing-remitting multiple sclerosis
RT	room temperature
SD	standard deviation
SEM	standard error of mean
SPMS	secondary-progressive multiple sclerosis
TCR	T-cell receptor
Th cells	T helper cells
Ti:Sa	titan:saphire
TNF	tumor necrosis factor
TPLSM	two-photon laser scanning microscopy
Treg	regulatory T-cell
Tuj1	beta-III tubulin
UV	ultraviolet
w	weeks
WT	wildtype
ZNS	zentrales Nervensystem
β-ME	β-Mercaptoethanol
µl	microliter
µm	micrometer

LIST OF FIGURES AND TABLES

ZUSAMMENFASSUNG

Die Multiple Sklerose (MS) ist eine T-Zell-getriebene, chronisch-entzündliche Autoimmunerkrankung des zentralen Nervensystems (ZNS), die im Verlauf zu Demyelinisierung und Neurodegeneration führt. Die MS-Forschung hat in den vergangenen Jahrzehnten große Fortschritte gemacht und insbesondere die neuroimmunologische Grundlagenforschung hat eine große Bandbreite an krankheitsmodifizierenden Therapien hervorgebracht. Diese zielen jedoch hauptsächlich auf die Modulation des Immunsystems in der Peripherie ab. Begründet ist dies unter anderem dadurch, dass aktuell die zugrundeliegenden Mechanismen der Neuroinflammation direkt im ZNS, insbesondere die funktionellen Eigenschaften infiltrierender T-Zellen sowie deren Interaktion mit weiteren gewebsständigen Zellen im ZNS noch unzureichend erforscht sind. Die vorliegende Arbeit thematisiert die Charakterisierung von infiltrierenden, proinflammatorischen T-Zellen in ZNS-Läsionen mittels Durchflusszytometrie und Zwei-Photonen Mikroskopie während der experimentellen autoimmunen Enzephalomyelitis (EAE), sowie den Einfluss des Adhäsionsmoleküls ICAM-5 auf die T-Zell-APC Interaktion im ZNS-Parenchym. Wir untersuchen zunächst Einflussfaktoren auf den Krankheitsverlauf der Transfer-EAE bei dem besonders das *in vitro* Differenzierungsprotokoll der transferierten Effektor-T-Zellen eine Rolle spielt. Darüber hinaus konnten wir Effektor-T-Zellen mittels Zwei-Photonen Mikroskopie in murinen ZNS-Läsionen *in vivo* darstellen und diese anhand ihrer Bewegungseigenschaften und Zytokinproduktion charakterisieren. Wir zeigen, dass in das ZNS Parenchym eingewanderte Th17 Zellen einen Interferon (IFN)-γ-produzierenden, ex-Th17 Phänotypen annehmen. Diese Änderung des Zytokinprofils ist darüber hinaus mit einer Änderung der funktionellen Eigenschaften verbunden. Diese entsprechen bei ex-Th17 Zellen eher denen von Th1 Zellen. Außerdem haben wir die Rolle des interzellulären Adhäsionsmoleküls (ICAM)-5 auf die T-Zell-APC Interaktion untersucht. Wir konnten zeigen, dass dieses besonders in der progressiven Neurodegenration eine Rolle spielt. Zusammenfassend beschreibt die vorliegende Arbeit neue Erkenntnisse der Pathophysiologie der Effektor- T-Zell-vermittelten Neuroinflammation innerhalb des ZNS-Parenchyms.

SUMMARY

Multiple sclerosis (MS) is a T-cell driven chronic inflammatory demyelinating disease of the central nervous system (CNS) characterized by immune cell infiltration into the CNS parenchyma leading to an inflammatory cascade, which finally results in primary demyelination and neurodegeneration. MS research has come a long way in the past decades and extensive basic research in the last decades has led to the development of several disease modifying therapies (DMT), whose main target remains the immune system in the periphery. This lack of therapies having an effect directly at the lesion site is partly due to the poor understanding of the underlying mechanisms of neuroinflammation within the inflamed CNS tissue. Especially the interaction between T-cells as main initiators of the disease and other resident cells in the CNS has not been sufficiently investigated. This work focuses on T-cell characteristics and functional dynamics of effector T-cells at the lesion site as well as the underlying mechanisms of interaction with antigen-presenting cells within the CNS. We investigated which determinants influence onset and course of experimental autoimmune encephalomyelitis (EAE) and identified the *in vitro* differentiation protocol of effector T-cells prior to transfer as important factor. In addition, we visualized effector T-cells immediately within the lesion site using *in vivo* two-photon microscopy and characterized infiltrating T-cells based on their motility parameters and flow cytometry data. We show that the encephalitogenic Th17-cells acquire an IFN-γ-producing, ex-Th17 phenotype *in vivo*. This change in cytokine profile is associated with a change in functional dynamics of ex-Th17-cells in EAE lesions which is reflected by an alteration of motility parameters which resemble Th1- rather than Th17-cells. Moreover, we studied the role of intercellular adhesion molecule (ICAM)- 5 on the T-cell-APC interaction in the CNS and show a role for ICAM-5 in progressive neurodegeneration. In conclusion, this thesis gives new insight into the pathological processes of effector T-cell driven neuroinflammation within the inflamed CNS tissue.

INTRODUCTION

Multiple sclerosis and experimental autoimmune encephalomyelitis

Multiple sclerosis (MS) is a chronic inflammatory demyelinating disease of the central nervous system (CNS) leading to neurodegeneration and long-term neurological disability. More than two million people worldwide are affected by MS (3, 4), making it the most common demyelinating disease (5) and a frequent cause of non-traumatic disability in the young adult population (6). Patients are typically between 15 and 55 years at the time of initial presentation (5) with a maximum frequency of diagnosis at around 30 years of age (6). MS affects twice as many women as men (5). Prevalence increases with distance north or south of the equator (7). The prevalence is highest in northern Europe, southern Australia, and the middle part of North America (6). To date, the mechanisms underlying pathogenesis of MS remain unknown but both environmental exposure and genetic susceptibility have been shown to play a role in disease development (7). The risk of developing MS increases 100-fold to 190-fold if an identical twin is affected while the concordance rate is 25–30 % among monozygotic twins (5, 8, 9). This indicates that while genetic factors do contribute to an individual risk of developing MS, genetics alone fails to explain disease development. Migration studies have provided strong evidence concerning environmental exposure. It has been shown that migration before 15 years of age from a high-prevalence to a lower-prevalence area reduces the likelihood of developing MS while migration to a higher-prevalence area between 11 and 45 years of age increases the risk of developing MS (5, 10, 11). Typically, MS patients present with a first clinical demyelinating event affecting the optic nerve, brainstem or spinal cord (12-14). Symptoms depend on lesion site but commonly include visual impairment, paresthesia, ataxia, or muscle weakness (6). About 80 % of patients show a relapsing-remitting disease course (RRMS) characterized by periods of neurological symptoms (relapses) that alternate with symptom free phases (remission). Over time, 65 % of

all patients with RRMS transition to a secondary progressive course (SPMS) characterized by a consistent progression of neurologic dysfunction and brain atrophy with or without additional occurring attacks and without phases of remission (6, 15-17). A minority of patients (20 %) show a primary progressive disease course (PPMS) defined by progressive neurological impairment lasting longer than one year and beginning directly at disease onset without relapses (15, 18) **(Figure 1)**. To what extent these disease courses are based on different pathomechanisms is highly debated (19-22). The most widely used guideline for diagnosing MS is the McDonald criteria, originally proposed in 2001 and since then regularly revised according to new scientific evidence, with the latest revision in 2017 (23). In order to study the molecular mechanisms of MS, several murine models have been developed, the most commonly used being experimental autoimmune encephalomyelitis (EAE). The model was developed in 1933 by Rivers et al. (24) and shares many histopathological and immunological

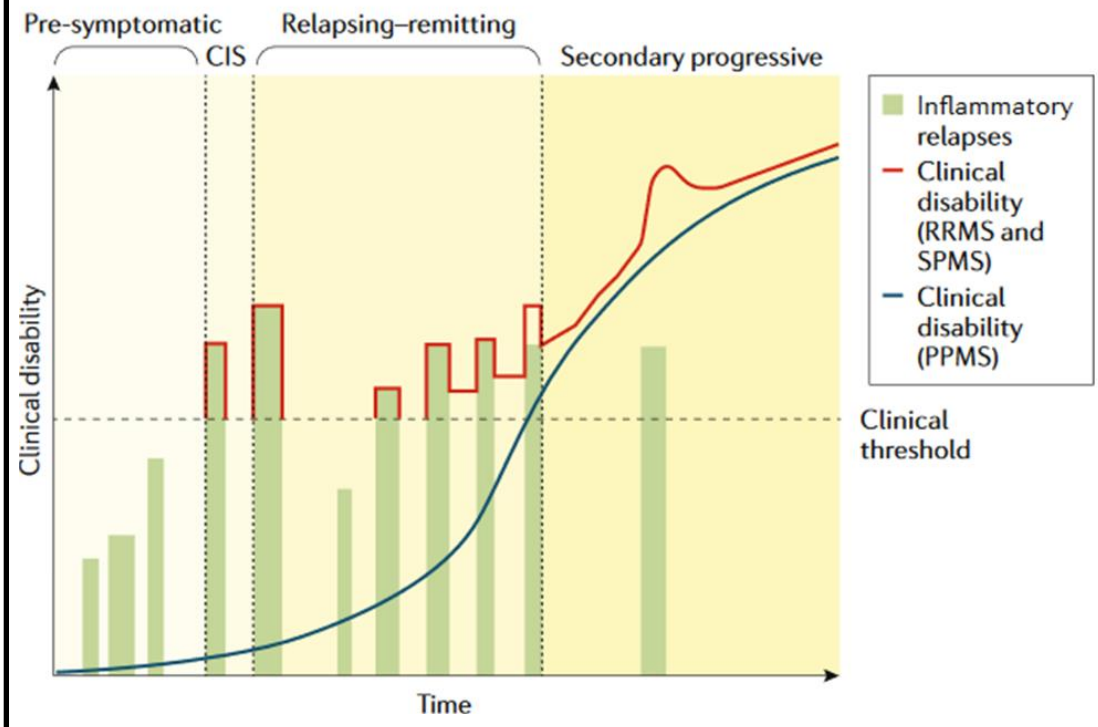

Figure 1 : Clinical course of MS
Clinical disability is shown over time in pre-symptomatic and CIS patients as well as in the three major forms of MS RRMS, SPMS (red) and PPMS (blue). Inflammatory relapses are marked in green. These may cross the clinical threshold, leading to symptoms and clinical relapse or remain below the threshold increasing clinical disability without clinical relapse. CIS: clinically isolated syndrome; MS: multiple sclerosis; RRMS: relapsing remitting MS; SPMS: secondary progressive MS; PPMS: primary progressive MS. Figure extracted from (2)

characteristics of MS (25, 26). Although the exact pathomechanisms remain unclear, the infiltration of active immune cells into the CNS is a well-defined characteristic of both MS and EAE (27, 28). As demyelination is a key feature of MS pathology, myelin protein-derived antigens such as myelin basic protein (MBP) or myelin oligodendrocyte glycoprotein (MOG) have been discussed to be the main autoreactive targets (28). Up to date, however, there is no dominant T-cell autoantigen defined in MS. This is in contrast to the animal model EAE, where it was clearly shown that myelin specific T-cells are the drivers of disease (29-32). Once activated, peripheral immune cells can cross the blood-brain barrier (BBB) (33), allowing further immune cell infiltration (34). Upon entering the CNS, the T-cells are reactivated by local and infiltrating activated antigen presenting cells (APC) which present major histocompatibility complex (MHC) class II-associated peptides (25). Reactivated T-cells lead to an inflammatory cascade, which finally results in primary demyelination and neurodegeneration (19, 21, 33, 34). Due to extensive research in the field, MS treatment has significantly improved in the last decades from pure symptom control over disease modification to current concepts of no evidence of disease activity (NEDA) and personalized treatment (35, 36). RRMS therapy concepts are characterized by early treatment and in cases of highly active MS, aggressive initial treatment (37-39) depending on patient characteristics such as pregnancy planning, compliance and comorbidities. Approved disease modifying treatments mainly target the immune system in the periphery. Although some have been shown to also have effects directly in the CNS in experiments, these effects are not completely understood to date (40). It is therefore crucial to better understand the underlying mechanisms of neuroinflammation directly at the lesion site in the inflamed CNS, not only to gain more insight into how currently approved therapies act within the CNS, but also for the development of new therapeutic strategies.

Effector T-cells

T-cells play a major role in the pathogenesis of EAE and MS (25). Over the years, various T helper cell subsets have been described, each defined by a unique cytokine profile and with different functional properties **(Figure 2)** (1).

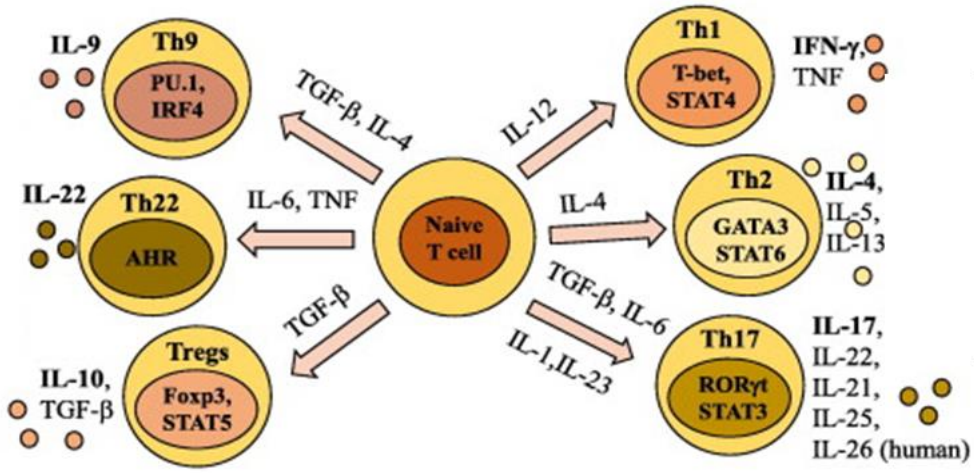

Figure 2: Differentiation of CD4$^+$ T-cell subsets
Naive T-cells primed by APCs can differentiate into Th1, Th2, Th17, Th9, Th22 or regulatory T-cells depending on the cytokine environment (arrows). The signature cytokines for each subset are shown in bold. STAT: Signal transducer and activator of transcription; RORγ: RAR related orphan receptor gamma, AHR: Aryl hydrocarbon receptor, Foxp3: forkhead box P3. Figure extracted from (1).

Both Th1- and Th17-cells have been shown to play a major role in development of EAE and MS, the exact pathomechanism of T-cell mediated neuroinflammation in the CNS tissue, however, remains a subject of research. Th1- cells are characterized by the secretion of IFN-γ and expression of the transcription factor T-bet and were originally thought to be the main pathogenic cells in EAE and MS (25, 41, 42). The discovery of IL-23 as critical cytokine for autoimmune neuroinflammation marked a turning point (43, 44), shifting the interest of research towards IL-17 secreting Th17-cells which express retinoid-related orphan receptors (ROR)γt (45-48). Th17-cells have been shown to enter the CNS via mechanisms different from Th1-cells and with different pathological phenotypes (49, 50). It has been proposed that IFN- γ-producing Th1-cells induce typical EAE, while IL-17-producing Th17-cells induce atypical EAE (51). Moreover, it has been shown that Th17-cells contribute to the first wave of attack

on the CNS leading to activation of microglia and secretion of proinflammatory cytokines even prior to disease onset (52, 53) and our lab provided mechanistic insights into Th17-cell-induced neuronal damage (54-56). Over the last years, it was increasingly recognized, that the distinction between the Th1 and Th17 subset in the context of neuroinflammation is not as clear as previously considered (57). It has been shown that encephalitogenic Th17-cells can display pathogenic features previously attributed to Th1-cells (58) and vice versa (59). Moreover, fate-mapping experiments demonstrated that Th17-cells in the CNS co-express or exclusively express IFN-γ (60, 61). This led to the conclusion that Th17-cells can switch to an IFN-γ-producing, ex-Th17 phenotype, that no longer produces IL-17. The molecular mechanisms of Th17-cell plasticity have been a subject of research and have been shown to be highly dependent on the tissue environment of the cells (62, 63). This is reflected in experiments which showed that Th17 acquire a Th1-like phenotype, upregulating T-bet and IFN-γ, in response to IL-12 or IL-23. Based on the observations of IFN-γ/IL-17A double-producing $CD4^+$ T-cells, Th17-cells may switch to a Th1 phenotype via an intermediate stage where the cell expresses both RORγt and T-bet and produce cytokines characteristic of Th17- and Th1-cells (64-68). The biological relevance of Th17 plasticity, as well as whether ex-Th17-cells functionally resemble Th1- or Th17-cells in the inflamed CNS tissue remains poorly understood.

Regulatory T-cells

Regulatory T-cells (Tregs) play a major role in maintaining immune homeostasis and tolerance to self-antigens. In both mice and humans, thymic-derived regulatory T-cells are characterized by high expression of the cytokine IL-2 receptor α-chain (CD25) and expression of the transcription factor FoxP3 (69-73). FoxP3 plays a central role for the development, maintenance and function of regulatory T-cells. Mutations of FoxP3 cause a fatal disorder

characterized by immune dysregulation, polyendocrinopathy, enteropathy and X-linked inheritance (IPEX) in humans (74). While it has been shown that MS patients show an enrichment of Tregs in the cerebrospinal fluid (CSF) compared to the peripheral blood (75, 76), the suppressive capacity of Tregs in RRMS patients is impaired compared to healthy controls (77). The involvement of regulatory T-cells in MS was further indicated by studies in EAE. Here it has been shown that regulatory $CD4^+$ cells prevent spontaneous EAE development (78) and that transfer of Tregs ameliorates EAE (79, 80). In addition, Tregs accumulate in the CNS during EAE (81, 82) and absence of Tregs promotes enhanced infiltration of lymphocytes from the periphery to the CNS (83).

Antigen presenting cells

MS as well as EAE are thought to be mediated by autoreactive T-cells directed against CNS-derived antigens (84). APCs are a heterogeneous group of cells involved in multiple stages during MS and EAE that process and present antigen via MHC class II to $CD4^+$ T-cells (85). Moreover, they provide secondary signals through the interaction of co-stimulatory molecules such as CD80 and CD86 with CD28 on T-cells (85). The initiation of the T-cell mediated adaptive immune response towards myelin-derived antigen is discussed to be induced by molecular mimicry in the periphery (86) or drainage of the respective CNS-antigen in soluble form or via APC- mediated delivery to deep cervical lymph nodes where antigens are presented to naïve T-cells (57, 87-90). Once primed and activated in the periphery, T-cells migrate towards the CNS where they can enter the CNS via the vessels of the choroid plexus or leptomeninges (57, 91, 92). After crossing this first barrier, T-cells in the perivascular space have to cross the glia limitans to enter the CNS parenchyma (93). In the perivascular space, professional APCs are present and likely to be involved in enabling T-cells to cross the glia limitans by presenting their cognate antigen (93). Within the CNS parenchyma various cell types such as dendritic

cells, microglia and astrocytes have been discussed to have the ability to present myelin-specific antigen to infiltrating T-cells under inflammatory conditions inducing their activation and proliferation (92). The exact underlying mechanisms of T-cell-APC interactions within the inflammatory lesion, however, remain a topic of research (85, 88, 91, 92).

Adhesion molecules

In the pathogenesis of MS or EAE, adhesion molecules are not only involved in the migration process of lymphocytes into the CNS parenchyma via the blood-brain barrier (94-96), they also contribute to the reactivation of immune cells via APCs. Moreover, adhesion molecules have been shown to be involved in direct T-cell interactions with neurons *in vivo*, inducing cell-cell contact-mediated neuronal calcium elevations (54, 56, 94). One well-investigated example of an adhesion molecule from the immunoglobulin superfamiliy is ICAM-1, which is typically expressed on endothelial and immune cells, and which can be induced by inflammatory cytokines such as IL-1 and tumor necrosis factor (TNF) α. Upon activation, leukocytes can bind to endothelial cells via lymphocyte function-associated antigen (LFA)-1/ICAM-1 and transmigrate into CNS tissue (97). In contrast, the CNS-specific ICAM-5, belonging to the same family of adhesion molecules, was first described as a regulator for brain development and the formation of synapses and is exclusively expressed on neurons in the telencephalon (98). The binding partner of ICAM-5 is LFA-1, which is expressed by invading leukocytes. LFA-1/ICAM-5 binding has therefore been proposed to play a role in neuroinflammatory processes in the CNS by enabling T-cells to directly bind to neurons (99, 100). Additionally, ICAM-5 can be cleaved by matrix metalloproteinase (MMP)-2 and 9 from the neuronal surface (101). This soluble form (sICAM-5) has been proposed to act as an inhibitor of ICAM-1–LFA-1 interactions between $CD4^+$ T-cells and APCs thereby inhibiting co-stimulatory signaling and full reactivation of $CD4^+$ T-cells (102, 103).

Two-photon laser scanning microscopy

Two-photon laser scanning microscopy (TPLSM) allows high-resolution, high-sensitivity fluorescence microscopy in intact neural tissue (104, 105). The technique was first described by Denk et al. in 1990 (106) and provides several advantages when compared to conventional single-photon confocal microscopy, such as the possibility to perform three-dimensionally resolved imaging of living cells within strongly scattering samples like the murine brain (107). In neuroscience, TPLSM has been widely used to study calcium dynamics (108, 109) and to perform long-term imaging of neurodevelopment (107, 110, 111). Moreover, TPLSM allows visualizing immune cell dynamics and cell-cell-interactions within the CNS in both homeostasis and inflammation. The ability to visualize immune cells within the CNS *in vivo* has led to new insights into the role and function of these cells. Using two-photon microscopy it has been shown that microglia are highly active also in their presumed resting state, continually surveying their microenvironment with extremely motile processes and protrusions (112). Moreover, drivers of $CD4^+$ T-cell migration in both healthy and inflamed CNS tissue could be identified (113-115) and real-time interaction between effector T-cells and cerebral structures were monitored using TPLSM (116).

Aim of the work

As described above, effector T-cells are the main drivers of autoimmune neuroinflammation in EAE and MS. However, the high plasticity of the Th17 subset, which in the context of neuroinflammation is able to acquire pathogenic features originally attributed to Th1-cells, makes a strict separation between Th1- and Th17-cells in the context of EAE difficult and has led to previous conflicting results concerning the differential contribution of Th1- and Th17-cells in EAE. In this work, we investigate the impact of effector T-cell differentiation on the EAE disease course. Moreover, we assess the cytokine profile and functional dynamics of both encephalitogenic Th1- and Th17-cells in the inflamed CNS using genetically encoded reporter mice, flow cytometry and intravital two-photon laser scanning microscopy. In addition, we investigate the role of adhesion molecule ICAM-5 and its suggested dual role in neuroinflammation using murine T-cell and neuronal cultures which we analyzed using flow cytometry, histology and qPCR. Moreover, we use ELISA of CSF samples of MS patients to assess its role in the human system.

MATERIAL AND METHODS

Material

Reagents, buffers and chemicals

Reagent	Company
4',6-Diamidino-2-phenylindole dihydrochloride (DAPI)	Sigma-Aldrich Corp., St Louis (USA)
Albumin bovine, cell culture grade (BSA)	Serva Electrophoresis GmbH, Heidelberg (Germany)
Ammonium chloride (NH4Cl)	Sigma-Aldrich Corp., St Louis (USA)
Aqua bi. dest. sterile	B. Braun AG, Melsungen (Germany)
Brefeldin A	Sigma-Aldrich Corp., St Louis (USA)
Carboxyfluorescein succinimidyl ester (CFSE)	Life Technologies Corp., Carlsbad (USA)
$CD4^+$ T-Cell Isolation Kit mouse	Miltenyi Biotec GmbH, Bergisch Gladbach (Germany)
Collagenase Typ IV	Sigma-Aldrich Corp., St Louis (USA)
Collagenase/Dispase	Roche, Mannheim (Germany)
D-Glucose	Carl Roth GmbH, Karlsruhe (Germany)
Dimethyl sulfoxide (DMSO)	Sigma-Aldrich Corp., St Louis (USA)
DNase-I	Roche, Mannheim (Germany)
DuoSet ELISA Ancillary Reagent Kit 2	R&D Systems, Minneapolis (USA)
EDTA disodium salt dehydrate (Na_2EDTA) solution (0.5 M)	Sigma-Aldrich Corp., St Louis (USA)
Ethanol 70 %	AppliChem GmbH, Darmstadt (Germany)
Ethylenediaminetetraacetic acid (EDTA)	Carl Roth GmbH, Karlsruhe (Germany)
FACSClean	BD Biosciences (Heidelberg
FACSFlow	BD Biosciences (Heidelberg)
FACSRinse	BD Biosciences (Heidelberg
Fetal Bovine Serum, heat inactivated (FBS)	Biochrom AG, Berlin (Germany)
Ficoll® Paque Plus	GE Healthcare, Chicago (USA)
Heat Inactivated Horse Serum (HI HS)	Life Technologies Corp., Carlsbad (USA)
Human ICAM-5 DuoSet ELISA	R&D Systems, Minneapolis (USA)
iQ™ SYBR® Green Supermix	Bio-Rad Laboratories, München (Germany)
Ketamine	Curamed (Germany)
L-Glutamine	Life Technologies Corp., Carlsbad (USA)
Lipopolysaccharide (LPS)	Enzo Life Sciences, Farmingdale (USA)
Magnesium chloride (MgCl2)	Sigma-Aldrich Corp., St Louis (USA)
MOG 35-55	GenScript Biotech, New Jersey (USA)
$NaHCO_3$	Carl Roth GmbH, Karlsruhe (Germany)
Normal Goat Serum	Vector Laboratories, Burlingame (USA)
Paraformaldehyde (PFA)	Carl Roth GmbH, Karlsruhe (Germany)
Penicillin/Streptomycin (P/S)	Life Technologies Corp., Carlsbad (USA)

Percoll	Sigma-Aldrich Corp., St Louis (USA)
Poly-L-lysine hydrobromide, average mol wt 30,000-70,000	Sigma-Aldrich Corp., St Louis (USA)
ProLong Gold Antifade Mountant	Thermo Fisher Scientific, Waltham (USA)
Propidium iodide (PI)	Sigma-Aldrich Corp., St Louis (USA)
Recombinant murine IFN-γ	Peprotech, Rocky Hill (USA)
RNaseOUT™ Recombinant Ribonuclease Inhibitor	Thermo Fisher Scientific, Waltham (USA)
RNeasy Mini Kit	Qiagen, Hilden (Germany)
sICAM-5 (ICAM-5 D1-2-Fc)	R&D Systems, Minneapolis (USA)
Superscript III First Strand Synthesis System	Thermo Fisher Scientific, Waltham (USA)
Triton-X	Sigma-Aldrich Corp., St Louis (USA)
Trypan blue	Sigma-Aldrich Corp., St Louis (USA)
Trypsin-EDTA (0.5%), no phenol red	Thermo Fisher Scientific, Waltham (USA)
Tween-20	Carl Roth GmbH, Karlsruhe (Germany)
Xylazinhydrochloride (2 %)	Bayer Health Care, Leverkusen (Germany)
β-Mercaptoethanol (β-ME)	Sigma-Aldrich Corp., St Louis (USA)

Buffer and media	**Company**
4-(2-hydroxyethyl)-1-piperazineethanesulfonic acid (HEPES)	Life Technologies Corp., Carlsbad (USA)
Basal Medium Eagle (BME)	Life Technologies Corp., Carlsbad (USA)
Dulbecco's Phosphate-buffered saline with Ca^{2+} & Mg^{2+} (PBS [+])	Sigma-Aldrich Corp., St Louis (USA)
Dulbecco's Phosphate-buffered saline without Ca^{2+} & Mg^{2+} (PBS [-])	Sigma-Aldrich Corp., St Louis (USA)
Dulbecco's Modified Eagle Medium (DMEM)	Life Technologies Corp., Carlsbad (USA)
Hank's Balanced Salt Solution (HBSS)	Thermo Fisher Scientific, Waltham (USA)
RPMI 1640 medium	Life Technologies Corp., Carlsbad (USA)
Neurobasal medium	Thermo Fisher Scientific, Waltham (USA)

Custom buffer and media	**Ingredients**
FACS buffer	PBS (+) + 5 g 0,5 % BSA

Lysis buffer	1000 ml Milli-Q-H_2O + 37,2 mg Na_2EDTA + 1 g $KHCO_3$ + 8,29 g NH_4Cl pH 7,2 -7,4
MACS buffer	PBS (+) + 5 g 0,5 % BSA + 4 ml 0,5M EDTA
Mouse medium	RPMI + 1 % HEPES 439,5 ml + 50 ml 10 % FCS + 5 ml 1 % L-Glutamin + 5 ml 1 % P/S + 0.5 ml 0.1 % ß-ME
Paraformaldehyde (PFA) buffer 4 %	40 g Paraformaldehyde + 1000 ml 0.1 M PBS buffer, pH 7.0 – 7.4
PBST	500 ml PBS [-] + 250 µl Tween-20
Saponin buffer	475 ml FACS buffer + 25 ml Saponin
Washing buffer	RPMI + 1 % Hepes 470 ml + 25 ml 5 % FCS + 5 ml 1 % P/S

Interleukins

Interleukin	**Company**
human TGF-β	R&D Systems, Minneapolis (USA)
IL-18	MBL, Woburn (USA)
IL-2	R&D Systems, Minneapolis (USA)
IL-23	R&D Systems, Minneapolis (USA)
IL-6	R&D Systems, Minneapolis (USA)

Antibodies

Antibody	Clone	Isotype	Company
αCD16/ αCD32 (FC-block)	2.4G2	rat-α-mouse monoclonal IgG2b, κ	BD Bioscience, Franklin Lakes (USA)
αCD25-APC	PC61	rat-α-mouse monoclonal IgG1, λ	BD Bioscience, Franklin Lakes (USA)
αCD28	H57-597	hamster-α-mouse monoclonal IgG2, λ1	BD Bioscience, Franklin Lakes (USA)
αCD3e	1452-C11	hamster-α-mouse monoclonal IgG1, κ	BD Bioscience, Franklin Lakes (USA)
αCD40L-PeCy7	MR1	hamster- α-mouse monoclonal IgG	BioLegend, San Diego (USA)
αCD44-AF700	IM7	rat-α-mouse monoclonal IgG2b, κ	Thermo Fisher Scientific, Waltham (USA)
αCD45-eFluor605	30-F11	rat-α-mouse monoclonal IgG2b κ	BD Bioscience, Franklin Lakes (USA)
αCD45-FITC	30-F11	rat-α-mouse monoclonal IgG2b κ	Thermo Fisher Scientific, Waltham (USA)
αCD49d-FITC	R1-2	rat-α-mouse monoclonal IgG2b, κ	Thermo Fisher Scientific, Waltham (USA)
αCD4-Horizon (V450)	RM4-5	rat-α-mouse monoclonal IgG2a, κ	BD Bioscience, Franklin Lakes (USA)
αCD4-PECy7	RM4-5	rat-α-mouse polyclonal IgG	BD Bioscience, Franklin Lakes (USA)
αCD54-APC	YN1/1.7.4	rat-α-mouse monoclonal IgG2b, κ	BioLegend, San Diego (USA)
αCD62L-APC	MEL-14	rat-α-mouse monoclonal IgG2a, κ	BD Bioscience, Franklin Lakes (USA)
αCD69-PE	H1.2F3	hamster- α-mouse monoclonal IgG1, λ3	BD Bioscience, Franklin Lakes (USA)
αGMCSF-PE	MP1-22E9	rat-α-mouse monoclonal IgG2a, κ	Thermo Fisher Scientific, Waltham (USA)
α-goat-AF568	polyclonal	donkey-α-goat polyclonal IgG [H+L]	Life Technologies Corp., Carlsbad (USA)
αI-A[b]-PE	AF6-120.1	mouse-α-mouse monoclonal IgG2a, κ	BD Bioscience, Franklin Lakes (USA)
αI-A[K]-FITC	10-3.6	mouse-α-mouse monoclonal IgG2a, κ	BD Bioscience, Franklin Lakes (USA)
αICAM-5	polyclonal	goat-α-mouse polyclonal IgG,	R&D Systems, Minneapolis (USA)
αIFN-γ	XMG1.2	rat-α-mouse monoclonal IgG1	BioXCell, West Lebanon (USA)
αIFN-γ-Horizon (V450)	XMG1.2	rat-α-mouse monoclonal IgG1, κ	BD Bioscience, Franklin Lakes (USA)
αIL-12	C17.8	rat-α-mouse monoclonal IgG2a	BioXCell, West Lebanon (USA)

αIL-17A-APC	17B7	rat-α-mouse monoclonal IgG2a, κ	Thermo Fisher Scientific, Waltham (USA)
αIL-4	1B11	rat-α-mouse monoclonal IgG1, κ	BioXCell, West Lebanon (USA)
αMAP-2	HM-2	mouse-α-mouse monoclonal IgG1	Sigma-Aldrich Corp., St Louis (USA)
α-mouse-AF488	polyclonal	goat-α-mouse polyclonal IgG [H+L]	Life Technologies Corp., Carlsbad (USA)
α-mouse-AF647	polyclonal	goat-α-mouse polyclonal IgG [H+L]	Life Technologies Corp., Carlsbad (USA)
αNeuN	polyclonal	rabbit-α-mouse polyclonal IgG	Merck Millipore, Billerica (USA)
α-rabbit-AF488	polyclonal	goat-α-rabbit polyclonal IgG [H+L]	Life Technologies Corp., Carlsbad (USA)
αRFP	RF5R	mouse- α-mouse monoclonal IgG1	Thermo Fisher Scientific, Waltham (USA)
αTNFα-AF700	MP6-XT22	rat-α-mouse monoclonal IgG1, κ	BD Bioscience, Franklin Lakes (USA)
αTubulin β 3	TUJ1	mouse-α-mouse monoclonal IgG2a, κ	BioLegend, San Diego (USA)
αVβ11-FITC	RR3-15	rat-α-mouse monoclonal IgG2b, κ	BD Bioscience, Franklin

Instruments

Instrument	**Company**
Analog Vortex Mixer	VWR International GmbH, Darmstadt (Germany)
Autoclave Heraeus	Thermo Fisher Scientific, Waltham (USA)
BD FACS Canto II	BD Bioscience, Franklin Lakes (USA)
Binocular Microscope Leica 56D	Leica Mikrosysteme Vertrieb GmbH, Wetzlar (Germany)
Bold-Line series of stage top incubators	Okolab, Pozzuoli (Italy)
Cell Counting Chamber Neubauer improved	Brand, Wertheim (Germany)
Cell Culture Incubator	Binder GmbH, Tuttlingen (Germany)
Cell Culture Microscope, bright field	Hund, Wetzlar (Germany)
Centrifuge Heraeus Fresco 21	Thermo Fisher Scientific Inc., Waltham (USA)
Centrifuge Multifuge Heraeus XIR	Thermo Fisher Scientific Inc., Waltham (USA)
CM 1900 Cryotome	Leica Mikrosysteme Vertrieb GmbH, Wetzlar (Germany)
Confocal Laser Scanning System SP8	Leica GmbH, Wetzlar, (Germany)
Eppendorf Research Adjustable-volume Pipettes	Eppendorf GmbH, Wesseling-Berzdorf (Germany)
Fridges and Freezers	Liebherr, Bulle (Switzerland)
Horizontal Laminar Flow Hood Heraguard	Thermo Fisher Scientific Inc., Waltham (USA)
IKAMAG® REC-G Magnetic Stirrer	IKA-Werke, Staufen im Breisgau (Germany)
Infinite M200 Pro microplate reader	Tecan, Männedorf (Switzerland)

Leica HCX IRAPO L 25x/0.95 W objective	Leica GmbH, Wetzlar (Germany)
Magnetic Stand Ambion	Thermo Fisher Scientific, Waltham (USA)
MaiTai Laser (Ti:Sa)	Spectra Physics, Irvine (USA)
MidiMACS and QuadroMACS Separators	Miltenyi Biotec GmbH, Bergisch Gladbach (Germany)
Olympus BX51 WI upright microscope fitted with an Olympus XLUMPlanFI 20x/0.95 W objective	Olympus Soft Imaging Solutions GmbH, Münster (Germany)
Optical Parametric Oscillator (OPO)	APE, Berlin (Germany)
Pipetus	Hirschmann Laborgeräte GmbH & Co.KG, Eberstadt (Germany)
Surgery Instruments	Fine Science Tools Inc., Heidelberg (Germany)
Thermal Cycler	Peqlab GmbH, Erlangen (Germany)
TriMScope I 2-photon microscope	La Vision BioTec GmbH, Bielefeld (Germany)
Vertical Laminar Flow Hood SAFE 2020	Thermo Fisher Scientific Inc., Waltham (USA)
Water bath Aqualine AL18	Lauda GmbH & CO. KG, Lauda-Königshofen (Germany)

Labware and Equipment

Product	**Company**
6 Well Cell Clear Flat Bottom Surface-Modified Multiwell Culture Plate	Corning Inc., Corning (USA)
96-, 48-, 24-, 12-Well Multiwell Culture Plate	Greiner Bio-One GmbH, Frickenhausen (Germany)
Cell Culture Dish, polystyrene, Ø 60 mm + 100 mm	Greiner Bio-One GmbH, Frickenhausen (Germany)
Centrifuge Tubes, polypropylene (PP), 15 ml + 50 ml	Greiner Bio-One GmbH, Frickenhausen (Germany)
Eppendorf Tubes 1.5 ml + 2 ml	Eppendorf GmbH, Wesseling-Berzdorf (Germany)
Filter pipette tips 10 µL, 200 µL, 1000 µL	Starlab, Hamburg (Germany)
MACS LS Columns	Miltenyi Biotec GmbH, Bergisch Gladbach (Germany)
Microscope glass slides	Thermo Fisher Scientific Inc., Waltham (USA)
Multiplate PCR Plates, 96 Wells, clear	Bio-Rad Laboratories GmbH, München (Germany)
Nalgene Rapid-Flow Filter Unit, 500 ml	Thermo Fisher Scientific Inc., Waltham (USA)
Pipette tips	VWR International GmbH, Darmstadt (Germany)
Pre-Separation Filters, 30 µm	Miltenyi Biotec GmbH, Bergisch Gladbach (Germany)

Software

Software	Company
Fiji (ImageJ)	National Institutes of Health, Bethesda (USA)
GraphPad Prism 6	GraphPad Software, Inc., La Jolla (USA)
Office 2010	Microsoft Corp., Redmond (USA)
Imaris	Oxford Instruments, Abingdon (UK)
FACSDiva	BD Bioscience, Franklin Lakes (USA)
Beacon Designer 8 Software	Premier Biosoft International, Palo Alto (USA)
Bio-Rad CFX Manager	Bio-Rad Laboratories, München (Germany)
NanoDrop 2000/2000c Operating Software	Thermo Fisher Scientific, Waltham (USA)
FlowJo	Tree Star, Ashland (USA)
FACSDiva	BD Bioscience, Franklin Lakes (USA)

Mouse strains

Strain	Target Properties	Origin/Reference/In-house-breeding
Rag2.cgn	Mice have impaired T- and B-cell development	Mazurier et al., 1999 (117)
B6.IL17A-EGFP.acRFP x 2d2	$CD4^+$ T-cells are MOG35–55 specific and express red fluorescent protein, IL17A-producing cells express green fluorescent protein	B6.IL17A-EGFP was originally obtained from Jackson (#018472) B6.acRFP and B6.2d2 were bred in-house
C57BL/6 (B6)	wildtype mice	Janvier Labs, Laval (France)
B6.2d2	$CD4^+$ T-cells are MOG35–55 specific	Bettelli et al., 2003 (31)
B6.2d2.CFP	$CD4^+$ T-cells are MOG35–55 specific and express cyan fluorescent protein	B6.2d2 x B6.CFP
B6.2d2.RFP	$CD4^+$ T-cells are MOG35–55 specific and express red fluorescent protein	B6.2d2 x B6.RFP
B6.2d2.GFP	$CD4^+$ T-cells are MOG35–55 specific and express green fluorescent protein	B6.2d2 x B6.GFP

Methods

Cell culture

Isolation of primary murine naïve $CD4^+$ T-cells

Mice were sacrificed by cervical dislocation and spleens, axial and brachial lymph nodes were collected. Organs were meshed through a 100 µm cell strainer in order to create a single cell suspension. Cells were washed by adding washing medium to the suspension and centrifuged at 500 g for 5 minutes. Cells were subsequently lysed using 10 ml lysis buffer. Reaction was stopped by adding 5 ml washing medium. Cells were again centrifuged, supernatant was discarded and the pellet was taken up in MACS buffer for further procedure. Cell count was determined using a Neubauer chamber. All following steps were performed on ice. Magnetic labelling was performed by adding 40 µl MACS buffer and 10 µl of $CD4^+$ T-cell biotin-antibody cocktail per 10^7 cells. The mixture was incubated for 5 minutes at 4 °C. Subsequently, 30 µl of MACS buffer, 20 µl of anti-biotin beads and 5 µl of CD8-Ly2 beads per 10^7 cells were added and incubated for another 10 minutes at 4 °C. Before continuing with cell separation, 35 ml of MACS buffer were added followed by centrifugation at 550 g for 5 minutes. The cell pellet was resuspended in 1 ml MACS buffer. LS columns with 30 µl pre-separation filters were placed in a pre-cooled QuadroMACS separator and equilibrated by rinsing with 3 ml of MACS buffer. Subsequently, 1 ml of cell suspension was added to the column and flow-through was collected in a fresh 50 ml falcon. Falcons containing cell suspension were rinsed two times with 3 ml of MACS buffer. Lastly, LS columns were rinsed with 3 ml of MACS buffer. The entire 10 ml of flow-through were collected and used for further procedure. As a pre-sort MACS control, the pipette tip used to resuspend the cell pellet was resuspended in a 1.5ml tube filled with 1 ml of FACS buffer and later used for flow cytometry. Flow-through was centrifuged at 550 g for 5 minutes and supernatant was discarded. Subsequently, magnetic labelling of

$CD62L^+$ cells was performed by adding 960 µl of MACS buffer and 40 µl of CD62L beads independent of cell numbers and incubation for 15 minutes at 4 °C. Magnetic separation was performed as described above. After rinsing the LS column for the third time, columns were removed from the MACS separator and put on a 15 ml falcon. 5 ml of MACS buffer were added and pushed through the column. Flow-through containing $CD4^+CD62L^+$ naïve T-cells was collected and used for cell culture. 100 µl of flow through were used as a post-MACS control for flow cytometry.

Isolation of antigen presenting cells

For isolation of antigen presenting cells, wildtype mice were sacrificed by cervical dislocation, spleens were collected and meshed through a 100 µm cell strainer in order to create a single cell suspension. Cells were washed by adding washing medium to the suspension and centrifuged at 500 g for 5 minutes. Cells were subsequently lysed using 10 ml lysis buffer. Reaction was stopped by adding 5 ml washing medium. Cells were again centrifuged, supernatant was discarded and the pellet was taken up in MACS buffer for further procedure. Cell count was determined using a Neubauer chamber. All following steps were performed on ice. Magnetic labelling was performed by adding 95 µl MACS buffer and 5 µl of CD90.2 beads per 10^7 cells. The mixture was incubated for 15 minutes at 4 °C. Before continuing with cell separation, 35 ml of MACS buffer were added followed by centrifugation at 550 g for 5 minutes. The cell pellet was resuspended in 1 ml MACS buffer. LS columns with 30 µl pre-separation filters were placed in a pre-cooled QuadroMACS separator and equilibrated by rinsing with 3 ml of MACS buffer. Subsequently, 1 ml of cell suspension was added to the column and flow-through was collected in a fresh 50 ml centrifuge tube. Falcons containing cell suspension were rinsed two times with 3 ml of MACS buffer. Lastly, LS columns were rinsed with 3 ml of MACS buffer. The entire 10 ml of flow-through were collected and used for

further procedure. Cells were subsequently irradiated at 30 Gy and taken up in mouse medium for further procedure.

In vitro differentiation of T-cell subtypes

For Th17 differentiation 0.6 million naïve T-cells isolated as described above were plated with 5.4 million irradiated APCs in a 24-well cell culture plate. Culture medium was enriched with the following cytokines: 2 µg/ml αCD3, 3 ng/ml TGF-β, 20 ng/ml IL-23 and 20 ng/ml IL-6. After 3 and 5 days of culture, T-cells were split and culture medium enriched with 50 U/mL IL-2 and 10 ng/ml IL-23 was added to each well. Restimulation of cells was performed after 7 days of culture by co-culture of 1 million T-cells with 5 million freshly isolated irradiated APCs. 2 µg/ml αCD3, 0.75 ng/ml TGF-β, 20 ng/ml IL-23, and 10 ng/ml IL-6 were added. Three days after restimulation cells were used for induction of transfer EAE. For all other experiments Th17-cells were harvested after 5 days of culture.

For Th1 differentiation 1 million naïve T-cells isolated as described above were plated with 5 million irradiated APCs in a 24-well cell culture plate. Culture medium was enriched with the following cytokines: 2 µg/ml αCD3, 50 ng/ml IL-12, 25 ng/ml IL-18 and 10 µg/ml αIL-4. After 2 and 4 days of culture, T-cells were split and 1 ml culture medium enriched with 100 U/ml IL-2 was added to each well. Cells were harvested after 5 days of culture.

Proliferation assay

Carboxyfluorescein succinimidyl ester (CFSE) proliferation assay was performed by incubating naïve T-cells in mouse-medium at 37 °C for 30 min, then cells were washed twice with pre-warmed RPMI+1 % HEPES (RH) and then dissolved in CFSE in pre-warmed RH at a concentration of 2.5 µM. After quenching the stained cells with cold mouse-medium, cells were incubated for at least 72 hours and evaluated by flow cytometric measurements.

Neuronal culture

For neuronal cultures, P0-P1 pups were decapitated and brains were removed from the skull. Preparation was performed in cold HBSS. Olfactory bulbs, meninges and hippocampus were removed from the cortex. Cortices from up to three animals were pooled into one falcon of cold HBSS. The tissue was washed once with cold HBSS and digested in HBSS with 1 % DNAse and 0.5 % trypsin for 20 min at 37 °C. Subsequently, the tissue was sucked through two small glass pipettes and poured over a 70 µm cell sieve for homogenization. For histology, 75,000–150,000 cells/well were seeded in DMEM with 1 % Pen/Strep, 10 % FBS and 2 mM L-glutamine on a 24 well plate with glass cover slips coated with poly-L-lysine. The next day, cells were washed and washing was then performed every two to three days. For qPCR, 500,000–750,000 cells per well were seeded in a 6-well plate. Neuronal cultures were inflamed between d7 and d8 with LPS (10 µg/ml), IFN-γ (100 ng/ml) or splenocyte supernatant and harvested 24 hours later. Cells were harvested with 3 % trypsin for 5 minutes at 37 °C, washed from the plates and collected on ice. The cells were centrifuged for 5 minutes at 550 g at 4 °C and washed once with cold PBS. Pellets for mRNA analysis were frozen at -80 °C.

Flow cytometry

Flow cytometry is a common method to analyze cell numbers, morphological features and expression of both cell surface and intracellular or intranuclear markers. Morphological characteristics are assessed by interpretation of the light scattering mediated by the cell structures. Cell markers are labelled using fluorochrome-conjugated antibodies and cells are run through the cytometer in a single cell suspension where bound fluorochromes are excited by their corresponding wavelength emitted by laser beams. After excitation the emitted signal is detected and converted to a digital signal. A FACS Canto II was used for all experiments in this thesis. The optics of the analyzer consist of an excitation source with three different lasers.

Eight different fluorescent molecules can be detected in addition to cell size (forward scatter) and cell granularity (sideward scatter). Acquisition of data was performed using FACS Diva software, analysis of the data was performed using FlowJo software.

Surface staining

For surface staining cells were taken up in 1 ml FACS buffer in a 1.5 ml Eppendorf tube and subsequently centrifuged at 500 g for 5 minutes. Next, the pellet was resuspended in 100 µl of FACS buffer with added fluorochrome-conjugated antibodies directed to the target antigens in the appropriate dilution and incubated for 10 minutes at 4 °C. Cell suspension was then washed with FACS buffer and either directly analyzed by flow cytometry or further proceeded performing intracellular or intranuclear staining.

Intracellular staining

For intracellular staining, surface stained cells were fixed by adding 500 µl of PBS and 500 µl of 4 % PFA to the cell pellet and incubated for 20 minutes at 4 °C in the dark. Subsequently, cells were permeabilized by washing with saponin buffer and supernatant was discarded. The cell pellet was then resuspended in 70 µl of saponin buffer containing a 1:70 dilution of αCD16/αCD32 antibody. After 10 minutes of incubation at 4 °C, 20 µl of staining mix containing saponin buffer and fluorochrome-conjugated antibodies directed against intracellular antigens was added to the mixture, vortexed and incubated for another 20 minutes at 4 °C. Lastly, cells were washed by adding 1 ml of FACS buffer and taken up in 200 µl of FACS buffer for flow cytometry analysis.

Quantitative real-time PCR

RNA was isolated using the RNeasy Mini Kit according to the manufacturer's protocol. Quality and integrity of total RNA was evaluated using a NanoDrop 2000c spectrophotometer. For cDNA synthesis, 1 µg of RNA was mixed with random hexamer primers and SuperScriptIII First

Strand Synthesis System was used according to the manufacturer's instructions. Amplification primers for real-time PCR analysis were designed using the Beacon Designer 8 Software according to the manufacturer's guidelines and tested for amplification efficiency and specificity. Real-time PCR was performed using iQ SYBR Green supermix in an CFX Connect TM Real Time Detection System. Primer sequences: ICAM-5 (forward: CGTATGTATTGTTCGCTCTC; reverse: TTATTGAAGGGAATGGGTAGA) and MMP-9 (forward: AAGTCTCAGAAGGTGGAT; reverse: AATAGGCTTTGTCTTGGTA). Relative changes in gene expression were determined using the Ct method (118) with β-actin as reference gene.

Immunohistochemistry

Primary cell cultures were fixed using 4 % paraformaldehyde for 20 min at room temperature and washed 3 times in PBS. Subsequently, blocking was performed in PBS containing 0.3% Triton-X and 5% Normal Goat Serum for one hour at room temperature. Blocking solution was removed and primary antibodies diluted in blocking solution were added. Incubation of primary antibodies was performed at 4 °C over night. The following day, cells were washed 3 times in PBS and the according secondary antibodies in blocking solution were added. Incubation was performed for 3 hours at room temperature. Subsequently, cells were washed 3 times in PBS and DAPI staining was performed for 13 minutes at room temperature. After a last washing step, cover slips were transferred and embedded onto object plates.

Microscopy

<u>Intravital two-photon laser microscopy</u>

To perform intravital two-photon microscopy, mice were anesthetized using isoflurane. Mice were continuously ventilated using 1.5 % isoflurane via a facemask to maintain anesthesia during the procedure. Once anaesthetized, the head of the mice was shaved and disinfected using 70 % ethanol. Heartrate, breathing frequency and oxygenation was monitored during

surgery and imaging using a sensor at the foot of the mouse. Temperature was monitored and kept between 35-37 °C during the procedure. The depth of anesthesia was controlled by continuous CO_2 measurements of exhaled gas. Mice were placed onto a heated custom build surgery and microscopy table. The head was fixed and inclined to allow access to the brainstem. The musculature of the dorsal neck and the dura mater were removed. Subsequently, a sterile agarose patch (0.5 % in 0.9 % NaCl solution) was installed on the brain surface, which was used to capture the PBS bath used for immersion imaging that was continuously exchanged by a peristaltic pump. Dual near-infrared and infrared excitation of the brainstem was applied at 850 nm by an automatically tunable Ti:Sa laser and at 1110 nm by an optical parametric oscillator (OPO) pumped by the Ti:Sa laser. Volumes of approximately 300 µm x 300 µm x 72 µm were acquired over time using an Olympus XLUMPlanFI 20x/0.95 W objective on a TriMScope I from LaVision Biotec.

Video analysis

Video analysis was performed using Imaris software. Videos were cropped to be 20 minutes long and noise reduction was achieved using the software's medium filter. Cell tracks were created using the Imaris tracking tool and manually corrected. Track correction and verification was performed manually with 3D rotation. Contact duration between cell types was manually determined using 3D rotation.

Confocal microscopy

Neuronal cultures were imaged using a Leica confocal scanning system SP8. Laser excitation wavelengths were set according to the used secondary antibodies. Additionally, the UV laser was used with a power of 0.5 %. Laser configurations were kept constant during all experiments. Acquired z-stacks were analyzed using FIJI software.

Animal experiments

All animal experiments were approved by local authorities and conducted according to the German Animals Protection Law for care and use of experimental animals. All animals were raised and kept in individually ventilated cages under specifically pathogen-free conditions at the University Medical Center of the Johannes Gutenberg University Mainz.

Experimental autoimmune encephalomyelitis (EAE)

To induce active EAE 6-8 week old mice were injected subcutaneously with 200 µl of myelin oligodendrocyte protein (MOG) 35-55 in complete Freund´s adjuvant (CFA). Mice received 200 ng of pertussis toxin (PTX) intraperitoneal at 0 and 24 hours after EAE induction. To induce adoptive transfer EAE, Rag2 $^{-/-}$ mice were used as recipient mice. Th17-cells were differentiated from naïve $CD4^{+}CD62L^{+}$ T-cells of donor mice for 10 days. Cells were harvested, counted and washed in PBS (+) three times. 10 million Th17-cells in 200 µl of PBS (+) were transferred by intravenous injection into the tail vein of the recipient mice. Following induction of EAE, clinical symptoms and weight were monitored daily staring on day 7 (active EAE) or day 10 (adoptive transfer). Clinical symptoms were translated to a clinical score from 0 to 5.

Clinical score	Typical EAE	Atypical EAE
0	no detectable sign of EAE	no detectable sign of EAE
0.5	tail weakness or hind limb weakness	
1	complete tail paralysis or loss of righting reflex	unsteady walk, mild ataxia
2	partial hind limb paralysis	ataxia, head tilt
2.5	unilateral complete hind limb paralysis	
3	bilateral complete hind limb paralysis	severe ataxia
3.5	complete hind limb paralysis and partial forelimb paralysis	
4	complete hind limb and forelimb paralysis	moribund
5	moribund or day after death	

Mice with a clinical score of 2 or higher were offered wet food and were injected with 200 µl of 5 % glucose subcutaneously. Mice losing more than 20 % of initial weight or with a score of 4 or higher were killed by cervical dislocation.

Perfusion and work-up of EAE mice

Mice were lethally anesthetized with an intraperitoneal injection of ketamine/xylazine. Depth of anesthesia was controlled by checking reflexes of the mouse. The abdomen was disinfected with 70 % ethanol and opened with scissors. The diaphragm and sternum were removed to access the heart. Subsequently, a 20G needle was inserted to the left ventricle and the right atrium was cut open. 30 ml of PBS were injected into the left ventricle to flush out blood. After perfusion, CNS and spinal cord were removed and transferred to IMDM for further procedure.

CNS was homogenized using a scalpel and subsequently digested with 50 µL collagenase (5 mg/µL), 50 µL collagenase/dispase (1000 U/µL) and 50 µL DNase (1 mg/mL) for 30 min at 37 °C. The mixture was then meshed through a 100 µm cell strainer and washed with IMDM. The cell pellet was then resuspended in 5 ml 30 % Percoll and carefully layered onto 5 ml of 70 % Percoll in a 15 ml falcon. After centrifugation at 750 g for 30 minutes without break, the interphase was removed and transferred to mouse medium. Cell suspension was subsequently centrifuged at 550 g for 5 minutes and either stained for surface FACS analysis or plated on a αCD3/αCD28 coated 96-well round bottom plate and stimulated for 4 hours for intracellular FACS analysis.

Statistical analysis

All data was analyzed using GraphPad Prism 6 software. Data are show as mean ± standard error of the mean unless stated otherwise. Statistical analysis was performed as parametric (student's t-test or ANOVA followed by Tukey's multiple comparison test) or non-parametric (Mann-Whitney-U test or Kruskal-Wallis test followed by Dunn's multiple comparison test) depending on passing Shapiro-Wilk normality test. *$p<0.05$.

RESULTS

EAE courses are highly dependent on *in vitro* differentiation and transfer protocols

In a first step, we analyzed protocols from the literature and identified aspects with a high variability between different laboratories (50, 51, 119-122), in order to assess how changes in protocol influence the onset and course of EAE. We identified the *in vitro* differentiation protocol, especially cytokine addition, as a possible modulating factor for further assessment. For the subsequent experiments, Th1- and Th17-cells were differentiated from naïve $CD4^+CD62L^+$ T-cells isolated from spleens of 2d2 donor mice **(Figure 3)**.

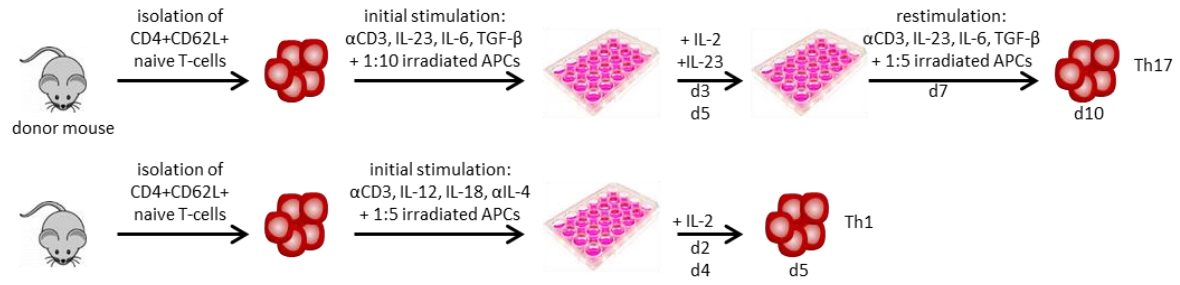

Figure 3: Experimental protocols to skew naïve $CD4^+CD62L^+$ towards Th17- or Th1-cells.

A major difference in differentiation protocols of Th1-cells in literature is the use of IL-18, a pro-inflammatory cytokine which has been shown to enhance the IL-12 driven Th1 immune response (123). In a first experiment, we therefore performed the differentiation of Th1-cells with or without addition of 25 ng/ml IL-18. When transferred into recipient mice, Th1-cells differentiated with IL-18 caused earlier onset of disease as well as stronger disease symptoms **(Figure 4A).** Next, we evaluated the role of IL-17 for disease development. To this aim, we correlated the IL-17 production of $CD4^+$ cells as measured by flow cytometry prior to transfer in recipient mice and the day of disease onset which was defined as day on which the first mouse showed EAE symptoms. We found a statistically significant correlation between IL-17 production and day of disease onset **(Figure 4B)**. Mice which received Th17-cells with a higher IL-17 production on the day of transfer, showed symptoms of EAE significantly earlier. Subsequently, we directly compared the difference between Th1- and Th17-induced transfer

EAE by transferring 10 million Th1-or Th17-skewed cells into recipient mice. Th1-induced EAE showed an earlier day of onset and earlier worsening of symptoms compared to Th17-induced EAE, but mice reached similar EAE scores **(Figure 4C)**. Previously, Th1 EAE has been associated with typical symptoms such as ascending paralysis, while Th17 EAE was associated with atypical symptoms such as brainstem and cerebellar symptoms showing as ataxia (51). There was indeed a clear trend towards more cases of atypical EAE symptoms in Th17-induced

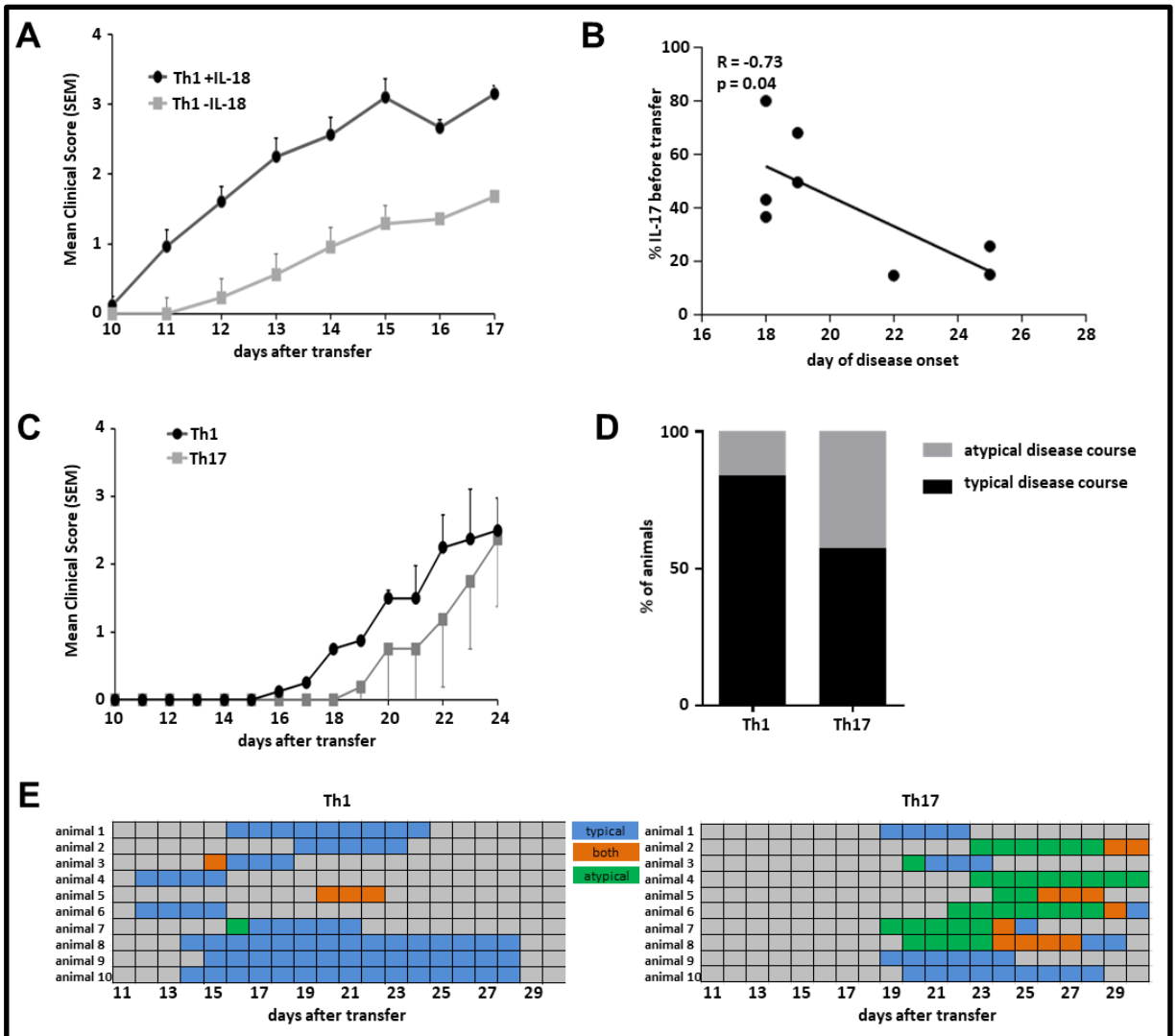

Figure 4: EAE courses depend on T-cell differentiation and transfer protocols
(A) IL-18 increases pathogenicity of Th1-cells. Animals were injected with Th1-cells differentiated with (black line) or without IL-18 (grey line). n = 12 animals per group. Mean clinical score and SEM shown. **(B)** IL-17 expression levels correlate with the onset of disease symptoms. Data from eight independent EAEs shown. Day of disease onset marks day of first mouse showing EAE symptoms. IL-17 production was measured on the day of transfer using flow cytometry. Line marks linear regression; Spearman's r is provided. **(C)** Disease courses dependent on Th1 or Th17 application. One representative experiment shown, n = 6 animals per group. **(D)** Quantification of typical and atypical disease courses upon Th1 or Th17 application. Data from at least four independent experiments with group sizes of 25-40 animals. **(E)** Representative examples of disease courses of individual mice.

transfer EAE, while atypical symptoms also occurred in some Th1 mice **(Figure 4D)**. Notably, mice that had received Th17-cells frequently showed atypical EAE symptoms at the beginning of disease, which later transitioned to typical EAE symptoms. This phenomenon was not observed in Th1-induced EAE **(Figure 4E)**.

Encephalitogenic Th17-cells acquire an ex-Th17 IFN-γ-producing phenotype *in vivo*

In vivo two-photon microscopy is a powerful tool to unravel inflammatory processes directly within the tissue (54, 116). To visualize T-cell infiltration within CNS lesions in living mice, Th1- and Th17-cells from 2d2.RFP mice and IL-17-reporter mice were differentiated following the protocol shown in **Fig. 3A** and transferred to Rag $2^{-/-}$ recipient mice **(Figure 5A).** Cells were monitored in the inflamed CNS at the peak of disease using TPLSM **(Figure 5B)**. Of note, we

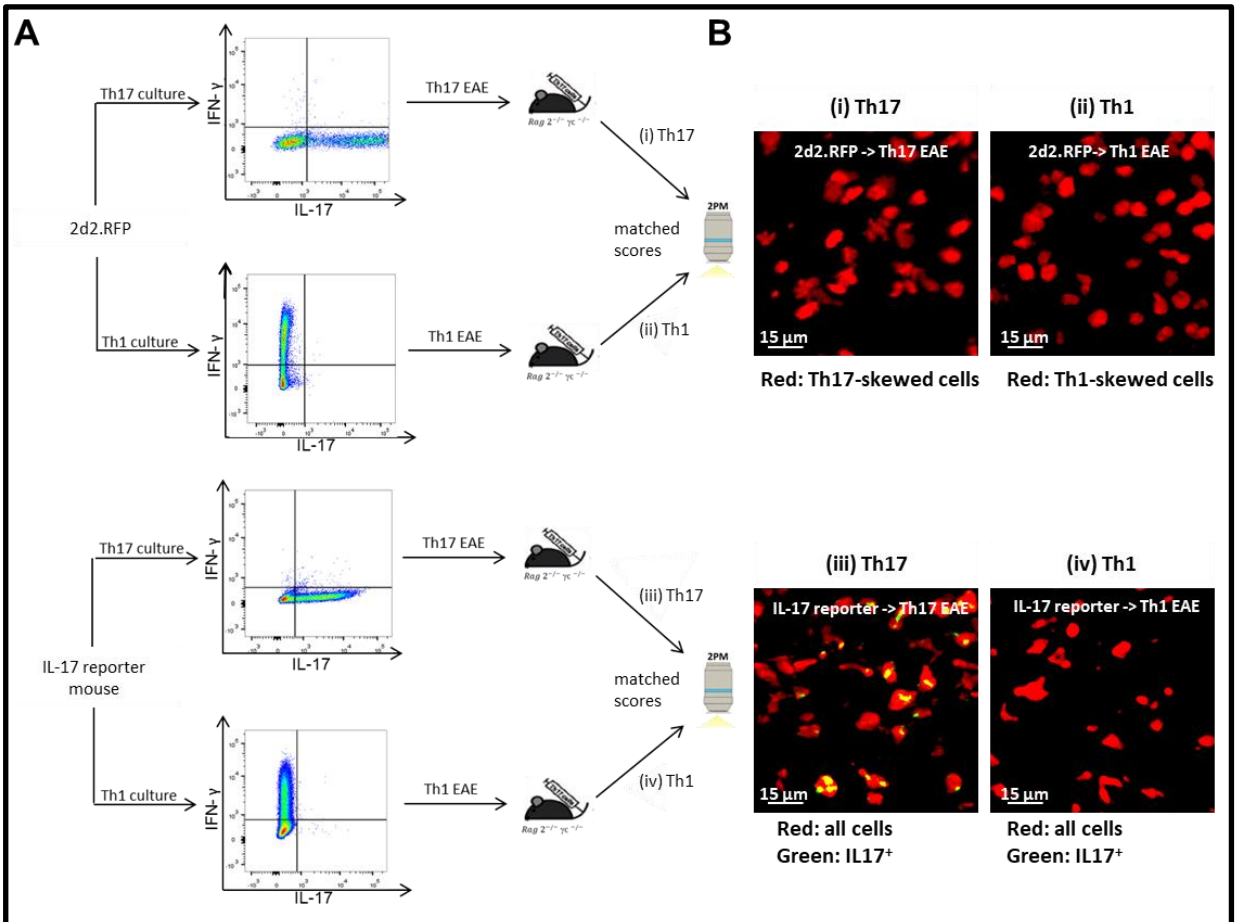

Figure 5: Visualization of encephalitogenic effector T-cells *in vivo*
(A) Experimental setup for TPLSM experiments. Naïve T-cells from 2d2.RFP or IL-17 reporter mice were skewed to Th1- or Th17-cells. Flow cytometry was performed to verify appropriate cytokine profile. Cells were transferred to recipient mice **(B)** Representative snapshots from TPLSM videos of different conditions. (i) transfer of 10 million 2d2.RFP Th17-skewed cells (ii) transfer of 10 million 2d2.RFP Th1-skewed cells (iii) transfer of 10 million IL17-reporter Th17-skewed cells (iv) transfer of 10 million IL17-reporter Th1-skewed cells

found similar cell numbers of Th17-and Th1-skewed cells in the CNS. In addition, we found statistically significantly lower levels of IL- 17 producing Th17-skewed cells and as expected no IL-17 producing Th1-cells **(Figure 6A)**. To determine the cytokine profile of Th1- and Th17- skewed 2d2.RFP cells within the CNS lesions, T-cells were isolated from the CNS and their cytokine profile was analyzed using flow cytometry, when animals reached a clinical score of two. Th1- cells showed a stable IFN-γ production and did not express IL-17. Th17-cells started to co-express IFN-γ in addition to their IL-17 production. IFN-γ expression levels in Th17-cells were comparable to levels in Th1-cells, underlining the acquisition of an ex-Th17 phenotype. This indicates that the majority of 2d2.RFP-derived cells monitored in our TPLSM experiments are IFN-γ producers. **(Figure 6B)**. The IFN-γ expression levels in Th17-cells

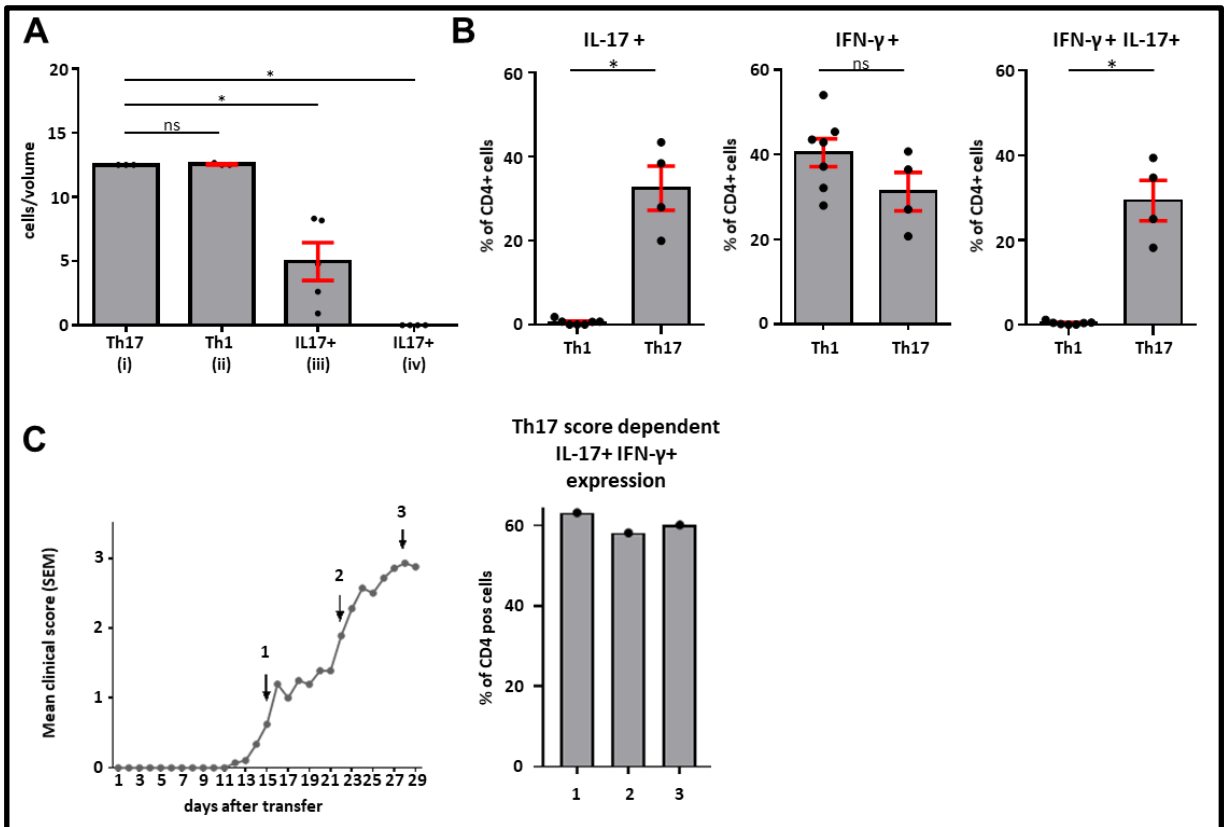

Figure 6: Encephalitogenic Th17-cells acquire an IFN-γ-producing phenotype *in vivo*
(A) Quantification of cells per area in videos from different conditions described in **Figure 5B**. Data from at least 3 different mice per condition shown. **(B)** Quantification of single cell, living $CD4^+$ cells after either Th1 or Th17 application. Animal scores were above 2. *$p<0.05$, n = 4-7 animals per group. **(C)** Representative disease of 14 mice from two independent experiments. IFN-γ expression (right) during Th17-induced disease (left). Expression levels of IFN-γ in ex-Th17 were measured when mice displayed clinical scores of 1, 2 and 3. Expression levels have already reached their maximum level at the onset of disease and remain stable over its course. n = 3

reached their maximum expression level at the beginning of disease and remained stable over time **(Figure 6C).**

Ex-Th17-cells show functional dynamics similar to Th1-cells but different from Th17-cells in the inflamed CNS tissue

We subsequently assessed the motility parameters of Th17-, ex-Th17- and Th1-cells in the CNS tissue. Ex-Th17-cells were defined as Th17-differentiated cells which showed no detectable IFN-γ production on the day of transfer, but started producing IFN-γ after infiltrating into the CNS as measured by flow cytometry. We found significant differences between Th17- and Th1- cells in displacement rate, mean track speed and track straightness indicating different functions exerted by the cell types within the tissue. Th1-cells moved slower, less straight and with a lower displacement rate than Th17-cells. Of note, ex-Th17-cells showed a motility significantly different from Th17-cells, but similar to Th1-cells **(Figure 7A-C)**.

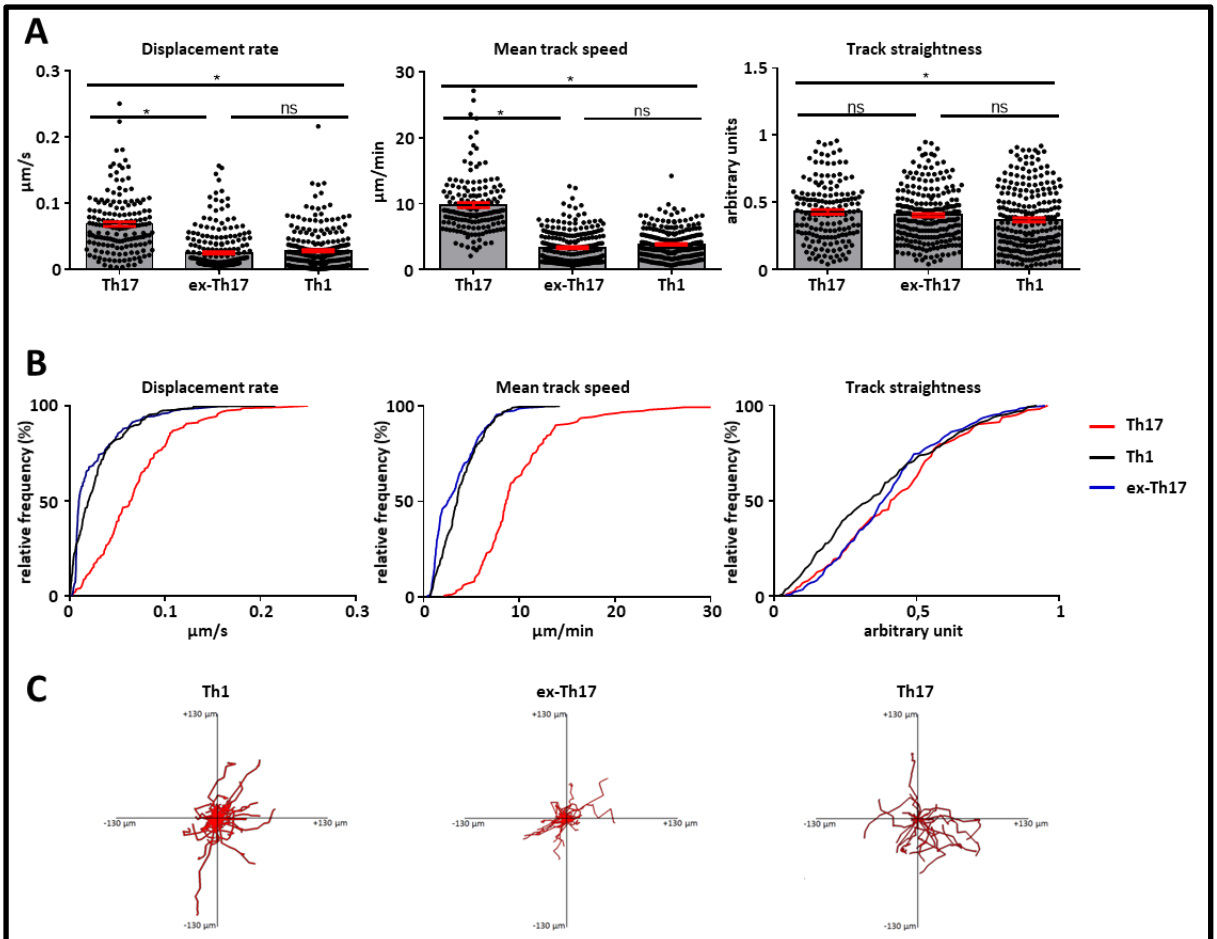

Figure 7: Ex-Th17 cells resemble Th1-cells in terms of motility *in vivo*

(A) Motility parameters of Th17, ex-Th17 and Th1-cells *in vivo*. Th17: IL-17 producing cells as indicated by IL- 17 reporter mouse. Ex-Th17: 2d2.RFP Th17-skewed cells. Th1: cells 2d2.RFP Th1-skewed cells. Displacement rate (displacement length divided by track duration), mean track speed and track straightness shown for different cell types. Data from at least 3 independent animals per group. *p<0.05, one-way ANOVA. **(B)** Relative frequency distribution of displacement rate, mean track speed and track straightness of Th17- cells (red), Th1-cells (black) and ex-Th17-cells (blue). **(C)** Superimposed tracks of Th1-, ex-Th17- and Th1-cells. One representative experiment per condition shown

Soluble ICAM-5 has no impact on Th17-cell-APC interaction *in vitro*

The reactivation of infiltrating T-cells by local APCs in the CNS is a crucial factor enabling T-cells to exert their effector functions and thereby adding to their pathogenicity (92). A proposed mechanism for the effect of adhesion molecule sICAM-5 is the competition of sICAM-5 with ICAM-1 expressed on effector T-cells for LFA-1 expressed on local APCs. By this means, the costimulatory signal induced by ICAM-1 for T-cell activation is neutralized which leads to the prevention of reactivation of effector T-cells and decreases their pathogenicity (103) **(Figure 8).**

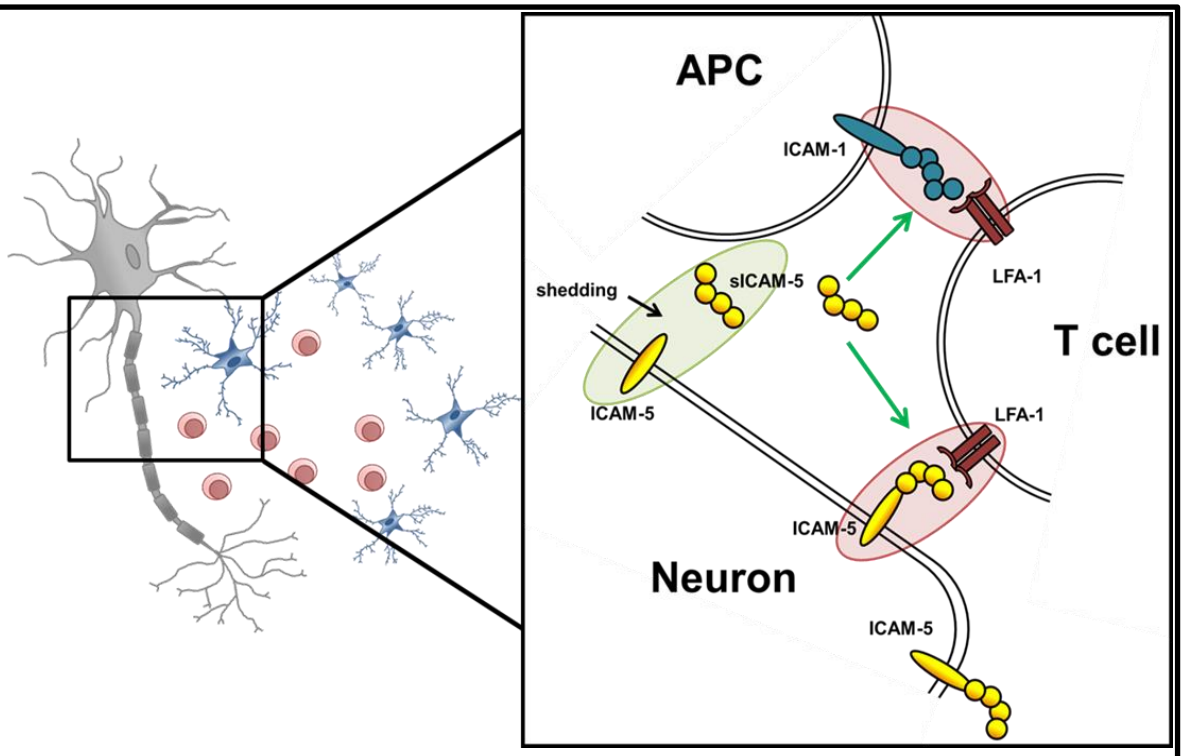

Figure 8: Schematic overview of potential ICAM-5 dependent T-cell – neuron and T-cell – APC interactions in the CNS
The adhesion molecule ICAM-5 (yellow) is expressed on neurons and can be shedded by MMP-2 and 9 from the neuronal surface. The soluble form sICAM-5 has been proposed to act as an inhibitor of ICAM1–LFA-1 interactions between T-cells and APCs and T-cells and neurons thereby displaying a protective function. Green highlights and arrows represent anti-inflammatory functions while red highlights represent proinflammatory properties. (125)

In order to evaluate a potential additional direct impact of sICAM-5 on effector T-cell function, we investigated the impact of sICAM-5 on the interaction of autoreactive T-cells with APCs *in vitro*. In a first step, we evaluated the expression level of its binding partner LFA-1 on T-cells.

There was no statistically significant difference in expression levels as measured by flow cytometry between naïve T-cells, Th17-skewed cells and stimulated Th17-skewed cells **(Figure 9A)**. Subsequently, we investigated the impact of sICAM-5 on the APC-dependent proliferation of Th17-cells and found no differences in the proliferation between the sICAM- 5-treated T-cells and control conditions **(Figure 9B)**. Moreover, sICAM-5 did not have an influence on the

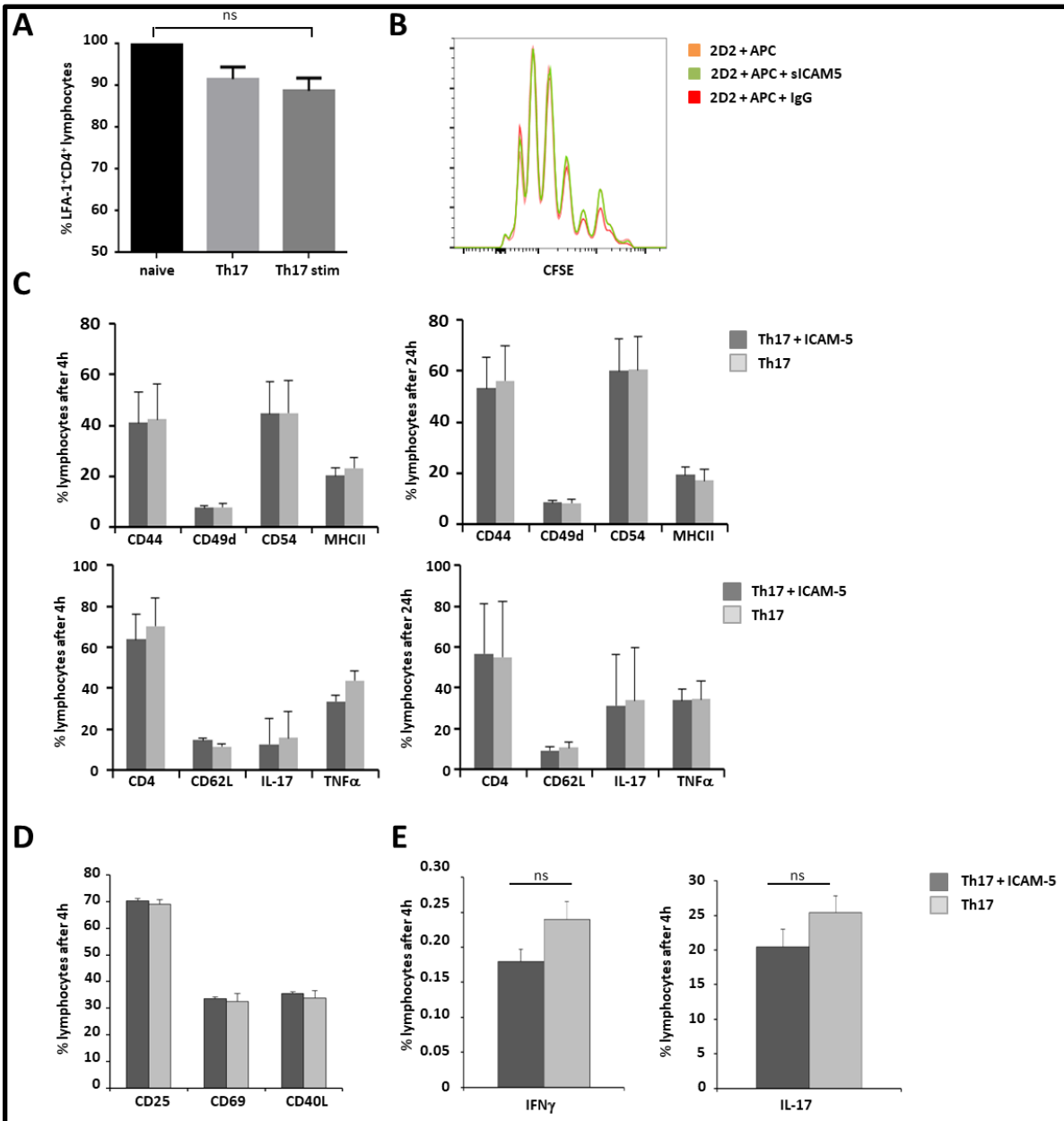

Figure 9: sICAM-5 does not affect Th17 - APC interactions

(A) FACS staining for LFA-1 of naïve T-cells, Th17-cells and Th17-cells after 24 h of stimulation with anti-CD3/CD28 n = 3. One-way ANOVA **(B)** Representative depiction of CFSE staining of naïve 2d2 T-cells co-cultured with APCs and sICAM-5 (10 µg/ml) or IgG (10 µg/ml) for 72 h. **(C)** FACS staining of Th17-cells stimulated for 4 h and 24 h with anti-CD3/CD28 and with or without ICAM-5 treatment (10 µg/ml). **(D,E)** Naïve T-cells were differentiated into Th17-cells with or without sICAM-5 treatment (10 µg/ml) and stained for extracellular (D) and intracellular (E) markers. (C-E) Data shown are mean ± SEM, Student's t-test. (125)

expression of CD44, CD49d, CD54, MHC class II, CD62L, IL-17 or TNFα after 4 or 24 hours of stimulation with anti-CD3/CD28 and sICAM5 on differentiated Th17-cells **(Figure 9C)**. In addition, we assessed the effect of sICAM-5 on the differentiation of naïve T-cells into Th17-cells. We did not find statistically significant differences in the expression of surface markers CD69, CD25, CD40L or intracellular cytokine levels for IL-17 and IFN-γ **(Figure 9D-E)**. In conclusion, these results indicate that sICAM-5 does not mediate its effect via altering the differentiation and function of murine Th17-cells.

ICAM-5 is expressed on cortical neurons and upregulated upon inflammatory stimuli

Subsequently, we investigated the expression and modulating factors of ICAM-5 in cortical neuronal cultures. To this aim, we cultured dissociated cortical neurons and stained them for NeuN and ICAM-5 and could confirm expression of ICAM-5 on protein level in cultured neurons (**Figure 10A**). Moreover, we investigated possible modulating factors of ICAM-5 and

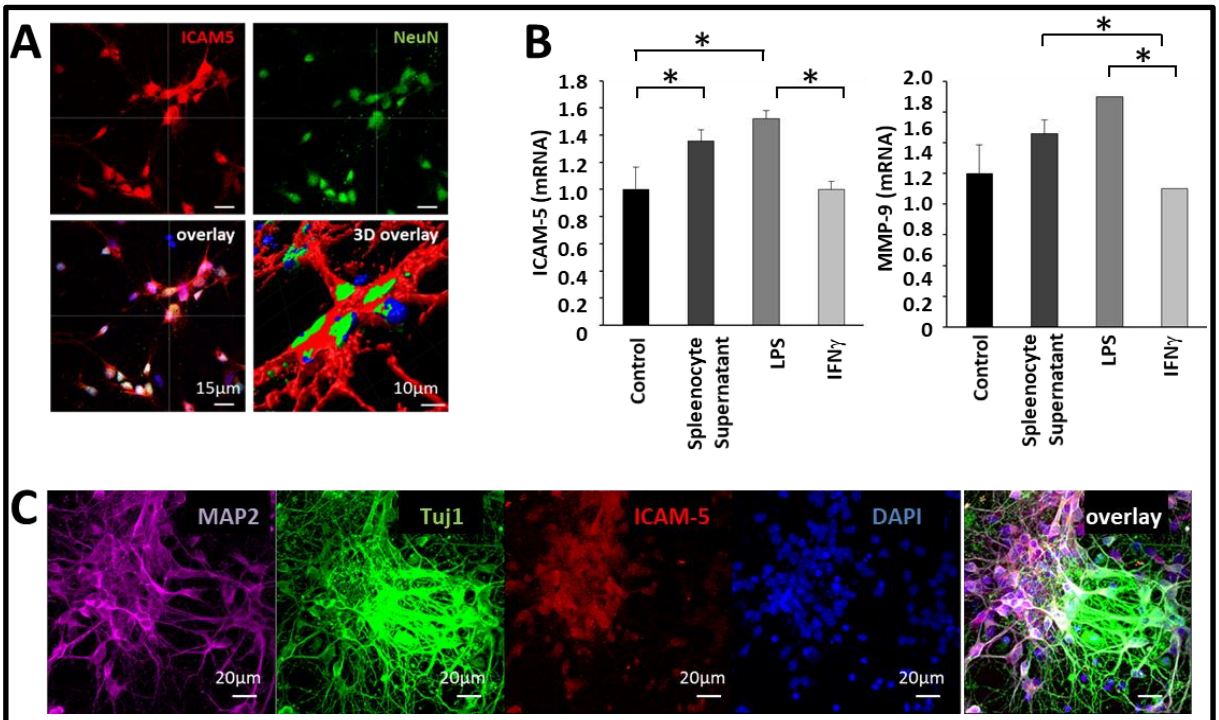

Figure 10: Expression of neuronal ICAM-5 in cortical neurons
(A) Immunohistochemical staining of ICAM-5-AF647 (red) on cortical neurons (scale bar = 15 µm, 3D overlay scale bar = 10 µm). Co-staining was performed with NeuN-AF488 (green) and DAPI (blue). **(B)** mRNA analysis of ICAM-5 and MMP-9 were performed with cortical neurons after stimulation with LPS, IFN-γ and splenocyte supernatant n = 6. Unstimulated cortical neurons served as a control. **(C)** Immunohistochemical staining of MAP2- AF647, Tuj1-FITC, ICAM-5-AF568 and DAPI on cortical neurons (scale bar = 20 µm). (125)

matrix metalloproteinase (MMP)-9, which is able to cleave ICAM-5 from the neuronal surface and has been shown to play a role in ICAM-5 dependent dendritic spine development (124). We found an upregulation of both ICAM-5 and MMP-9 after inflammatory stimulation with LPS and splenocyte supernatant, but not with IFN-γ (**Figure 10B**). Additional neuronal markers MAP-2 or beta-III tubulin (Tuj1) were used to stain cortical neurons and to validate that ICAM- 5 is preferentially expressed on soma and dendrites (102) (**Figure 10C**).

Patients suffering from progressive forms of MS show low levels of sICAM-5 in CSF

Our group had previously shown that ICAM-5 plays a major role in the progressive phase of EAE by showing statistically significant differences in EAE course between actively induced EAE in wildtype and ICAM-5 knockout (KO) mice (125). Based on these EAE findings, suggesting an endogenous protective role of sICAM-5, we investigated the role of sICAM-5 in the human system by assessing sICAM-5 levels in the CSF of MS patients. CSF samples from RRMS, SPMS and PPMS patients as well as from a control group (NIND) with normal CSF findings were analyzed using a human ICAM-5 ELISA. While RRMS and control patients showed comparable levels of sICAM-5, sICAM- 5 levels in PPMS and SPMS patients were statistically significantly lower **(Figure 11A)**. We moreover correlated sICAM-5 concentration in CSF with the EDSS score and disease duration **(Figure 11B)** for each MS patient subtype. In RRMS, we found a moderate correlation between EDSS and sICAM-5 concentration in the CSF with higher EDSS scores being associated with a lower concentration of sICAM-5 in the CSF. In SPMS and PPMS, we found a correlation between disease duration and sICAM-5 concentration with higher sICAM-5 concentrations correlating with longer disease duration.

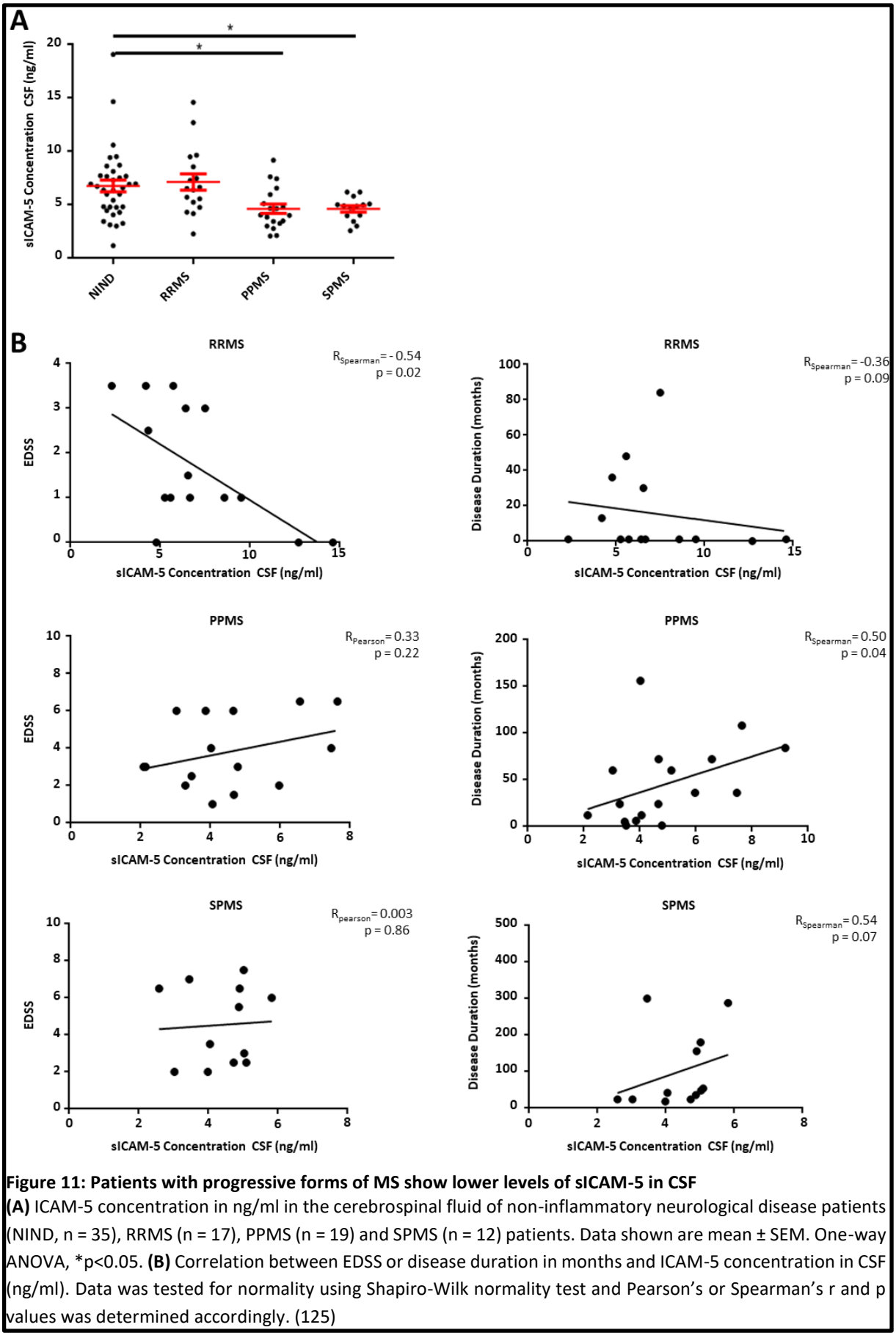

Figure 11: Patients with progressive forms of MS show lower levels of sICAM-5 in CSF
(A) ICAM-5 concentration in ng/ml in the cerebrospinal fluid of non-inflammatory neurological disease patients (NIND, n = 35), RRMS (n = 17), PPMS (n = 19) and SPMS (n = 12) patients. Data shown are mean ± SEM. One-way ANOVA, *p<0.05. **(B)** Correlation between EDSS or disease duration in months and ICAM-5 concentration in CSF (ng/ml). Data was tested for normality using Shapiro-Wilk normality test and Pearson's or Spearman's r and p values was determined accordingly. (125)

DISCUSSION

Pivotal contributions to MS research have been made using the EAE model. It is the most commonly used animal model to investigate MS and shares key immunopathological and neuropathological features such as inflammation and resolution of inflammation, demyelination and gliosis with the human disease (126). However, EAE protocols, especially for adoptive transfer EAE, are highly variable between laboratories (49-51, 119, 120, 127, 128). In this study, we therefore investigated how changes in EAE protocol contribute to alterations in the disease course. We identified cytokine addition to *in vitro* culture as a central aspect varying between laboratories. IL-12 is a common feature of all Th1 differentiation protocols analyzed and has been widely discussed and investigated in the context of Th1 differentiation. Previous murine studies indicated that IL-12 stimulation is sufficient to induce encephalitogenicity in $CD4^+$ cells suggesting a role for Th1- but not Th17-cells in EAE (59, 121). These findings, nevertheless, have been challenged by the ability to induce EAE in mice deficient in IL-12 (129) and the fact that donor T-cells had been derived from wildtype mice that could have been exposed to endogenous IL-23, which promotes Th17 function, in the donor mouse (59). Of note, due to the proposed role of IL-12 and IL-23 in EAE and its efficacy in the treatment of other autoimmune diseases such as psoriasis or Crohn's disease, the common IL12/IL-23 p40 subunit neutralizing antibody ustekinumab has been tested as a possible therapeutic approach in MS (130-132). In a multicenter, randomized, double-blind, placebo-controlled phase II study in RRMS patients, however, the antibody showed no efficacy in reducing the number of gadolinium-enhancing T1 lesions and no median change in EDSS (131). This was suggested to be due to insufficient penetration of ustekinumab to the target organ through the blood-brain barrier. The disrupted blood-brain barrier in MS lesions, however, should allow for at least part of the antibody to reach the CNS (132, 133). In addition,

specifically neutralizing the p40 subunit of IL-12 could lead to a pro-inflammatory shift in IL-12 signaling outweighing the effects of p40 neutralization (132). Moreover, other inflammatory pathways not affected by ustekinumab could be involved and explain the lack of efficacy in MS patients (133). Taken together, this data suggests that the role for cytokines in differentiation of T-helper cell subsets in neuroinflammation is not limited to the impact of IL-12 or IL-23 and that alternative pathways of cytokines contributing to T-cell pathology should be evaluated. In our study, we subsequently investigated the role of IL-18 for the differentiation of Th1-cells and its contribution to Th1-cell pathogenicity. The IFN-γ-inducing factor IL-18 (123) has been shown to play a role in both MS (134) and EAE (135, 136) and contribute to IFN-γ-induction in Th1-cells (123, 137, 138). Still, IL-18 was only partly used in the analyzed Th1 differentiation protocols. We compared the disease course of Th1-induced transfer EAE between mice that received Th1-cells differentiated with and without IL-18 addition. Notably, Th1-cells differentiated in presence of IL-18 induced higher clinical scores in recipient mice indicating that IL-18 increases pathogenicity of Th1-cells. Subsequently, the role of the effector T-cell subset on the EAE disease course was evaluated. To this end, the equal amount of Th1- or Th17-cells were transferred into recipient mice on the same day and disease courses between the two groups were compared. Of note, the T-cell subset transferred to recipient mice played a role only during the onset of the disease. Mice having received Th17-cells showed a later day of onset and slower acceleration of disease severity but reached similar EAE scores when compared to mice having received Th1-cells. This delay of disease activity could be explained by a possible need for Th17-skewed cells to acquire an IFN-γ-producing phenotype in order to show a similar pathogenicity as Th1-skewed cells. Although the exact pathophysiological role of ex-Th17-cells in the context of neuroinflammation is not fully understood, ex-Th17-cells in other diseases have been shown to be resistant to Treg-mediated suppression and, in the case of autoimmune arthritis,

constitute the majority of tissue infiltrating cells, indicating their pathogenic potential (139, 140). Previous studies suggested that atypical EAE symptoms mirrored by ataxia reflect Th17-driven disease while typical EAE symptoms characterized by ascending paralysis reflect Th1-driven disease (51). A switch in cytokine profile from IL-17 producing Th17-cells towards an IFN-γ-producing ex-Th17 phenotype could therefore be an explanation for the observed switch from atypical to typical EAE symptoms during Th17 transfer EAE. We additionally confirmed this hypothesis by performing flow cytometric analysis of CNS-localized effector T-cells. Here we observed high IL-17 IFN-γ co-expression at the beginning of the disease. These results are in line with the described highly context dependent Th17-plasticity enabling Th17-cells to acquire features originally contributed to other T-cell subsets depending on the environmental context (64-68, 141). In our study, we confirm that T-cells skewed towards Th17-cells *in vitro* acquire an IFN-γ-producing Th1-like phenotype *in vivo* based on flow cytometry experiments (46, 141). In addition to flow cytometric data, we show that IFN-γ-producing ex-Th17-cells functionally resemble Th1- rather than Th17-cells based on the functional dynamics of the cells in the CNS. Using intravital TPLSM and genetically encoded reporter mice, we were able to monitor the different T-cell subsets in the CNS *in vivo*. To this aim, we used 2d2.RFP mice and IL-17 reporter mice and induced Th1 and Th17 EAE. As described before, 2d2.RFP Th17-skewed cells acquired an IFN-γ-producing ex-Th17 phenotype allowing us to compare the motility of Th17-cells indicated by IL-17 reporter mouse, ex-Th17-cells and Th1-cells *in vivo*. Subsequently, effector T-cells in the CNS parenchyma were monitored using TPLSM and their behavior and functional dynamics as reflected by motility parameters were analyzed. In this set up, Th1-cells and ex-Th17-cells showed a motility behavior different from Th17-cells. They moved slower, less straight and with a lower displacement rate. These parameters are indicative of an increased cell-cell contact and higher pathogenicity (54). This contributes to previous reports claiming ex-Th17-cells unite various

detrimental properties highlighting their role for pathogenicity in autoimmunity (62). Moreover, it shows that the dogmatic distinction between Th1- and Th17-induced EAE is not useful in the context of neuroinflammation as ex-Th17-cells are able to exert functions similar to Th1-cells in the CNS. One limitation of our study is the definition of ex-Th17-cells. In our TPLSM experiments we monitor all Th17-skewed 2d2.RFP cells. Although we clearly show that the majority of Th17-skewed 2d2.RFP cells acquire IFN-γ production when infiltrating to the CNS, there are few cells included in our ex-Th17 group which do not produce IFN-γ. To further investigate the dynamics of ex-Th17-cells in the CNS it could therefore be of value to directly monitor IFN-γ-producing cells using a genetically encoded IFN-γ reporter mouse.

In MS, effector T-cells directly interact with neurons *in vivo* inducing neuronal damage via calcium elevations (54). In this aspect, ICAM-5 plays a dual role. It can serve as a binding partner for LFA-1 expressing, infiltrating leukocytes, by this means allowing for detrimental effects on neurons. At the same time, it can act as an endogenous regulator of neuronal damage by preventing neuron-T-cell and APC-T-cell contacts in its soluble form. The aim of our study was to investigate the role of ICAM-5 in Th17-mediated murine neuroinflammation and in MS. We could show that soluble ICAM-5 does not directly influence Th17 proliferation or cytokine expression in a murine *in vitro* assay. This is in contrast to previous studies (103) which were performed with $CD4^+$ cells in the human system. The contradicting results can be explained by the different organism in which experiments were performed but also by our more specific approach of investigating the influence of ICAM-5 on the interaction of Th17 differentiated $CD4^+$ cells with APCs. This raises the possibility that also in the human system the previously described effects are not due to a specific effect of ICAM- 5 on the Th17-APC interaction but rather due to interactions with other T-cell subtypes not further discriminated in the study. In contrast to ICAM- 1, which is mainly localized on glia and endothelial cells, ICAM-5 expression is restricted to telencephalic neurons (142). We therefore investigated the

expression and regulation of ICAM-5 on neurons in cortical neuronal culture. We confirmed an upregulation of both ICAM- 5 and MMP-9 under inflammatory conditions mimicked by stimulation of neuronal cultures with LPS or splenocyte supernatant. In contrast to ICAM-1 and in accordance with previous reports (103), we did not find an IFN-γ-dependent upregulation of shedded ICAM-5. Other proinflammatory cytokines included in the splenocyte supernatant, however, such as TNF-α could be involved in the upregulation and could be part of future investigations on the topic. Since we were able to exclude a direct effect of ICAM-5 on Th17-cell pathology we hypothesized that ICAM-5 might play a role in the interaction of neurons with APCs such as dendritic cells or microglia in EAE. Interestingly, LFA-1 is highly expressed by microglia in chronic active lesions (143) and can be bound by ICAM-5. This indicates a potential neuroprotective role of ICAM-5 especially in the chronic phase of MS and is in line with our previous findings that ICAM-5 plays a role especially during the chronic phase of EAE (125). Moreover, Paetau and colleagues showed that endogenous ICAM-5 from neurons is bound by microglia and induces clustering and weak adhesion of microglia (144). In addition, ICAM- 5 downregulates phagocytosis in microglia and promotes IL-10 production in LPS-stimulated microglia (144) indicating a neuroprotective role for ICAM-5 on neuron-APC interaction especially in chronic disease. In MS patients, CSF from patients suffering from a progressive form of MS show decreased ICAM-5 levels. This is in accordance with our previous murine data (125) and highlights the importance of ICAM-5 in the human system. Additionally, ICAM-5 concentrations in the CSF correlated with the disease duration in patients with progressive forms of MS. Previous studies showed that sICAM-5 is cleaved and released into the CSF also in other neurological diseases such as acute encephalitis (145). These findings raise interesting possibilities for further investigations as we could not classify the exact pathophysiological role of sICAM-5 release into the CSF in progressive MS patients. ICAM-5 has been discussed as a marker of neuronal death in traumatic brain injury (146), which

suggests that also increased levels of sICAM- 5 in MS patients could be caused by increased neuronal death during the disease course. The link between chronic disease, microglia activation and neuronal ICAM-5 (144), could also point towards other involved pathways in the correlation between sICAM-5 and disease duration. Interestingly, while we did not find a statistically significant difference in ICAM-5 levels between NIND and RRMS patients, there was a strong negative correlation between EDSS and ICAM-5 concentration in the CSF of RRMS patients, which supports our hypothesis.

Conclusion and outlook

In conclusion, we show that EAE onset and course is highly dependent on *in vitro* differentiation and transfer protocols used. We demonstrate that *in vitro* differentiated Th17-cells are able to acquire an IFN-γ-producing ex-Th17 phenotype in EAE using flow cytometry. Additionally, we found that these ex-Th17-cells show a behavior resembling Th1-cells rather than Th17-cells in EAE lesions *in vivo*. These results indicate that Th17-cells do not only alter their cytokine production when infiltrating to the CNS, but that the conversion is accompanied by a functional phenotype alteration of the cell with a potential increase in pathogenicity. In future studies, the pathophysiological role for ex-Th17, especially their interaction with CNS-resident glial cells as well as their pathogenicity and contribution to T-cell induced demyelination and neurodegeneration should be further addressed. Moreover, we showed that ICAM-5 does not alter APC-mediated Th17 proliferation and differentiation and that ICAM-5 is upregulated and increasingly shedded on neurons under inflammatory conditions. In humans, CSF from patients with progressive forms of MS show decreased sICAM-5 levels, suggesting a lack of the endogenous protective pathway in this patient group and pointing towards a novel role of ICAM-5 in progressive MS. In this context, especially the interaction

between ICAM-5, microglia and neurons as well as the underlying mechanisms for ICAM-5 shedding in chronic neuroinflammation merit further investigation.

ACKNOWLEDGEMENT

CURRICULUM VITAE

REFERENCES

1. Raphael I, Nalawade S, Eagar TN, Forsthuber TG. T cell subsets and their signature cytokines in autoimmune and inflammatory diseases. Cytokine. 2015;74(1):5-17.
2. Filippi M, Bar-Or A, Piehl F, Preziosa P, Solari A, Vukusic S, et al. Multiple sclerosis. Nature Reviews Disease Primers. 2018;4(1):43.
3. Feigin VL, Nichols E, Alam T, Bannick MS, Beghi E, Blake N, et al. Global, regional, and national burden of neurological disorders, 1990–2016: a systematic analysis for the Global Burden of Disease Study 2016. The Lancet Neurology. 2019;18(5):459-80.
4. Browne P, Chandraratna D, Angood C, Tremlett H, Baker C, Taylor BV, et al. Atlas of Multiple Sclerosis 2013: A growing global problem with widespread inequity. Neurology. 2014;83(11):1022-4.
5. Love S. Demyelinating diseases. J Clin Pathol. 2006;59(11):1151-9.
6. Noseworthy JH, Lucchinetti C, Rodriguez M, Weinshenker BG. Multiple sclerosis. N Engl J Med. 2000;343(13):938-52.
7. Compston A, Coles A. Multiple sclerosis. The Lancet. 2008;372(9648):1502-17.
8. Sadovnick AD, Dircks A, Ebers GC. Genetic counselling in multiple sclerosis: risks to sibs and children of affected individuals. Clin Genet. 1999;56(2):118-22.
9. Kenealy SJ, Pericak-Vance MA, Haines JL. The genetic epidemiology of multiple sclerosis. Journal of neuroimmunology. 2003;143(1-2):7-12.
10. Alter M, Leibowitz URI, Speer J. Risk of Multiple Sclerosis Related to Age at Immigration to Israel. Archives of Neurology. 1966;15(3):234-7.
11. Marrie RA. Environmental risk factors in multiple sclerosis aetiology. The Lancet Neurology. 2004;3(12):709-18.
12. Miller DH, Chard DT, Ciccarelli O. Clinically isolated syndromes. The Lancet Neurology. 2012;11(2):157-69.
13. Hou Y, Jia Y, Hou J. Natural Course of Clinically Isolated Syndrome: A Longitudinal Analysis Using a Markov Model. Scientific reports. 2018;8(1):10857.
14. Miller DH, Weinshenker BG, Filippi M, Banwell BL, Cohen JA, Freedman MS, et al. Differential diagnosis of suspected multiple sclerosis: a consensus approach. Multiple sclerosis (Houndmills, Basingstoke, England). 2008;14(9):1157-74.
15. Lublin FD, Reingold SC. Defining the clinical course of multiple sclerosis: results of an international survey. National Multiple Sclerosis Society (USA) Advisory Committee on Clinical Trials of New Agents in Multiple Sclerosis. Neurology. 1996;46(4):907-11.
16. Eshaghi A, Prados F, Brownlee WJ, Altmann DR, Tur C, Cardoso MJ, et al. Deep gray matter volume loss drives disability worsening in multiple sclerosis. Annals of neurology. 2018;83(2):210-22.
17. Compston A, Coles A. Multiple sclerosis. Lancet. 2008;372(9648):1502-17.
18. Thompson AJ, Banwell BL, Barkhof F, Carroll WM, Coetzee T, Comi G, et al. Diagnosis of multiple sclerosis: 2017 revisions of the McDonald criteria. The Lancet Neurology. 2018;17(2):162-73.
19. Larochelle C, Uphaus T, Prat A, Zipp F. Secondary Progression in Multiple Sclerosis: Neuronal Exhaustion or Distinct Pathology? Trends in neurosciences. 2016;39(5):325-39.
20. Lassmann H, van Horssen J. The molecular basis of neurodegeneration in multiple sclerosis. FEBS letters. 2011;585(23):3715-23.
21. Leray E, Yaouanq J, Le Page E, Coustans M, Laplaud D, Oger J, et al. Evidence for a two-stage disability progression in multiple sclerosis. Brain : a journal of neurology. 2010;133(Pt 7):1900-13.
22. Mahad DH, Trapp BD, Lassmann H. Pathological mechanisms in progressive multiple sclerosis. The Lancet Neurology. 2015;14(2):183-93.
23. Thompson AJ, Banwell BL, Barkhof F, Carroll WM, Coetzee T, Comi G, et al. Diagnosis of multiple sclerosis: 2017 revisions of the McDonald criteria. The Lancet Neurology. 2018;17(2):162-73.
24. Rivers TM, Sprunt DH, Berry GP. OBSERVATIONS ON ATTEMPTS TO PRODUCE ACUTE DISSEMINATED ENCEPHALOMYELITIS IN MONKEYS. J Exp Med. 1933;58(1):39-53.

25. Fletcher JM, Lalor SJ, Sweeney CM, Tubridy N, Mills KH. T cells in multiple sclerosis and experimental autoimmune encephalomyelitis. Clinical and experimental immunology. 2010;162(1):1-11.
26. Denic A, Johnson AJ, Bieber AJ, Warrington AE, Rodriguez M, Pirko I. The relevance of animal models in multiple sclerosis research. Pathophysiology : the official journal of the International Society for Pathophysiology. 2011;18(1):21-9.
27. Friese MA, Schattling B, Fugger L. Mechanisms of neurodegeneration and axonal dysfunction in multiple sclerosis. Nature reviews Neurology. 2014;10(4):225-38.
28. Dendrou CA, Fugger L, Friese MA. Immunopathology of multiple sclerosis. Nat Rev Immunol. 2015;15(9):545-58.
29. McMahon EJ, Bailey SL, Castenada CV, Waldner H, Miller SD. Epitope spreading initiates in the CNS in two mouse models of multiple sclerosis. Nat Med. 2005;11(3):335-9.
30. Rangachari M, Kuchroo VK. Using EAE to better understand principles of immune function and autoimmune pathology. Journal of autoimmunity. 2013;45:31-9.
31. Bettelli E, Pagany M, Weiner HL, Linington C, Sobel RA, Kuchroo VK. Myelin oligodendrocyte glycoprotein-specific T cell receptor transgenic mice develop spontaneous autoimmune optic neuritis. J Exp Med. 2003;197(9):1073-81.
32. Anderson AC, Chandwaskar R, Lee DH, Sullivan JM, Solomon A, Rodriguez-Manzanet R, et al. A transgenic model of central nervous system autoimmunity mediated by CD4+ and CD8+ T and B cells. J Immunol. 2012;188(5):2084-92.
33. Engelhardt B. Molecular mechanisms involved in T cell migration across the blood-brain barrier. Journal of neural transmission (Vienna, Austria : 1996). 2006;113(4):477-85.
34. Biernacki K, Prat A, Blain M, Antel JP. Regulation of cellular and molecular trafficking across human brain endothelial cells by Th1- and Th2-polarized lymphocytes. Journal of neuropathology and experimental neurology. 2004;63(3):223-32.
35. Bevan CJ, Cree BA. Disease activity free status: a new end point for a new era in multiple sclerosis clinical research? JAMA neurology. 2014;71(3):269-70.
36. Rotstein D, Montalban X. Reaching an evidence-based prognosis for personalized treatment of multiple sclerosis. Nature reviews Neurology. 2019;15(5):287-300.
37. Comi G, Radaelli M, Soelberg Sørensen P. Evolving concepts in the treatment of relapsing multiple sclerosis. The Lancet. 2016.
38. Rae-Grant A, Day GS, Marrie RA, Rabinstein A, Cree BAC, Gronseth GS, et al. Practice guideline recommendations summary: Disease-modifying therapies for adults with multiple sclerosis: Report of the Guideline Development, Dissemination, and Implementation Subcommittee of the American Academy of Neurology. Neurology. 2018;90(17):777-88.
39. Montalban X, Gold R, Thompson AJ, Otero-Romero S, Amato MP, Chandraratna D, et al. ECTRIMS/EAN Guideline on the pharmacological treatment of people with multiple sclerosis. Multiple sclerosis (Houndmills, Basingstoke, England). 2018;24(2):96-120.
40. Rommer PS, Milo R, Han MH, Satyanarayan S, Sellner J, Hauer L, et al. Immunological Aspects of Approved MS Therapeutics. Frontiers in Immunology. 2019;10(1564).
41. Panitch HS, Hirsch RL, Haley AS, Johnson KP. Exacerbations of multiple sclerosis in patients treated with gamma interferon. Lancet. 1987;1(8538):893-5.
42. Wekerle H, Kojima K, Lannes-Vieira J, Lassmann H, Linington C. Animal models. Annals of neurology. 1994;36 Suppl:S47-53.
43. Cua DJ, Sherlock J, Chen Y, Murphy CA, Joyce B, Seymour B, et al. Interleukin-23 rather than interleukin-12 is the critical cytokine for autoimmune inflammation of the brain. Nature. 2003;421(6924):744-8.
44. Langrish CL, Chen Y, Blumenschein WM, Mattson J, Basham B, Sedgwick JD, et al. IL-23 drives a pathogenic T cell population that induces autoimmune inflammation. J Exp Med. 2005;201(2):233-40.
45. Kebir H, Kreymborg K, Ifergan I, Dodelet-Devillers A, Cayrol R, Bernard M, et al. Human TH17 lymphocytes promote blood-brain barrier disruption and central nervous system inflammation. Nature medicine. 2007;13(10):1173-5.

46. Kebir H, Ifergan I, Alvarez JI, Bernard M, Poirier J, Arbour N, et al. Preferential recruitment of interferon-gamma-expressing TH17 cells in multiple sclerosis. Annals of neurology. 2009;66(3):390-402.
47. Waisman A, Hauptmann J, Regen T. The role of IL-17 in CNS diseases. Acta neuropathologica. 2015;129(5):625-37.
48. Yang XO, Pappu BP, Nurieva R, Akimzhanov A, Kang HS, Chung Y, et al. T helper 17 lineage differentiation is programmed by orphan nuclear receptors ROR alpha and ROR gamma. Immunity. 2008;28(1):29-39.
49. Rothhammer V, Heink S, Petermann F, Srivastava R, Claussen MC, Hemmer B, et al. Th17 lymphocytes traffic to the central nervous system independently of α4 integrin expression during EAE. The Journal of experimental medicine. 2011;208(12):2465-76.
50. Jäger A, Dardalhon V, Sobel RA, Bettelli E, Kuchroo VK. Th1, Th17, and Th9 effector cells induce experimental autoimmune encephalomyelitis with different pathological phenotypes. J Immunol. 2009;183(11):7169-77.
51. Domingues HS, Mues M, Lassmann H, Wekerle H, Krishnamoorthy G. Functional and pathogenic differences of Th1 and Th17 cells in experimental autoimmune encephalomyelitis. PLoS One. 2010;5(11):e15531.
52. Murphy AC, Lalor SJ, Lynch MA, Mills KH. Infiltration of Th1 and Th17 cells and activation of microglia in the CNS during the course of experimental autoimmune encephalomyelitis. Brain Behav Immun. 2010;24(4):641-51.
53. Alvarez JI, Saint-Laurent O, Godschalk A, Terouz S, Briels C, Larouche S, et al. Focal disturbances in the blood-brain barrier are associated with formation of neuroinflammatory lesions. Neurobiology of disease. 2015;74:14-24.
54. Siffrin V, Radbruch H, Glumm R, Niesner R, Paterka M, Herz J, et al. In vivo imaging of partially reversible th17 cell-induced neuronal dysfunction in the course of encephalomyelitis. Immunity. 2010;33(3):424-36.
55. Buehler U, Schulenburg K, Yurugi H, Solman M, Abankwa D, Ulges A, et al. Targeting prohibitins at the cell surface prevents Th17-mediated autoimmunity. The EMBO journal. 2018;37(16).
56. Paterka M, Siffrin V, Voss JO, Werr J, Hoppmann N, Gollan R, et al. Gatekeeper role of brain antigen-presenting CD11c+ cells in neuroinflammation. The EMBO journal. 2016;35(1):89-101.
57. Korn T, Kallies A. T cell responses in the central nervous system. Nat Rev Immunol. 2017;17(3):179-94.
58. Kara EE, McKenzie DR, Bastow CR, Gregor CE, Fenix KA, Ogunniyi AD, et al. CCR2 defines in vivo development and homing of IL-23-driven GM-CSF-producing Th17 cells. Nat Commun. 2015;6:8644.
59. Grifka-Walk HM, Giles DA, Segal BM. IL-12-polarized Th1 cells produce GM-CSF and induce EAE independent of IL-23. European journal of immunology. 2015;45(10):2780-6.
60. Kurschus FC, Croxford AL, Heinen AP, Wörtge S, Ielo D, Waisman A. Genetic proof for the transient nature of the Th17 phenotype. European journal of immunology. 2010;40(12):3336-46.
61. Hirota K, Duarte JH, Veldhoen M, Hornsby E, Li Y, Cua DJ, et al. Fate mapping of IL-17-producing T cells in inflammatory responses. Nat Immunol. 2011;12(3):255-63.
62. Basdeo SA, Cluxton D, Sulaimani J, Moran B, Canavan M, Orr C, et al. Ex-Th17 (Nonclassical Th1) Cells Are Functionally Distinct from Classical Th1 and Th17 Cells and Are Not Constrained by Regulatory T Cells. Journal of immunology (Baltimore, Md : 1950). 2017;198(6):2249-59.
63. Luger D, Silver PB, Tang J, Cua D, Chen Z, Iwakura Y, et al. Either a Th17 or a Th1 effector response can drive autoimmunity: conditions of disease induction affect dominant effector category. J Exp Med. 2008;205(4):799-810.
64. Morrison PJ, Ballantyne SJ, Kullberg MC. Interleukin-23 and T helper 17-type responses in intestinal inflammation: from cytokines to T-cell plasticity. Immunology. 2011;133(4):397-408.
65. Lee YK, Turner H, Maynard CL, Oliver JR, Chen D, Elson CO, et al. Late developmental plasticity in the T helper 17 lineage. Immunity. 2009;30(1):92-107.

66. Shi G, Cox CA, Vistica BP, Tan C, Wawrousek EF, Gery I. Phenotype switching by inflammation-inducing polarized Th17 cells, but not by Th1 cells. J Immunol. 2008;181(10):7205-13.
67. Lexberg MH, Taubner A, Albrecht I, Lepenies I, Richter A, Kamradt T, et al. IFN-γ and IL-12 synergize to convert in vivo generated Th17 into Th1/Th17 cells. European journal of immunology. 2010;40(11):3017-27.
68. Bending D, Newland S, Krejcí A, Phillips JM, Bray S, Cooke A. Epigenetic changes at Il12rb2 and Tbx21 in relation to plasticity behavior of Th17 cells. J Immunol. 2011;186(6):3373-82.
69. Sakaguchi S, Sakaguchi N, Asano M, Itoh M, Toda M. Immunologic self-tolerance maintained by activated T cells expressing IL-2 receptor alpha-chains (CD25). Breakdown of a single mechanism of self-tolerance causes various autoimmune diseases. J Immunol. 1995;155(3):1151-64.
70. Fontenot JD, Gavin MA, Rudensky AY. Foxp3 programs the development and function of CD4+CD25+ regulatory T cells. Nat Immunol. 2003;4(4):330-6.
71. Hori S, Nomura T, Sakaguchi S. Control of regulatory T cell development by the transcription factor Foxp3. Science (New York, NY). 2003;299(5609):1057-61.
72. Khattri R, Cox T, Yasayko SA, Ramsdell F. An essential role for Scurfin in CD4+CD25+ T regulatory cells. Nat Immunol. 2003;4(4):337-42.
73. Dominguez-Villar M, Hafler DA. Regulatory T cells in autoimmune disease. Nature Immunology. 2018;19(7):665-73.
74. Bennett CL, Christie J, Ramsdell F, Brunkow ME, Ferguson PJ, Whitesell L, et al. The immune dysregulation, polyendocrinopathy, enteropathy, X-linked syndrome (IPEX) is caused by mutations of FOXP3. Nature Genetics. 2001;27(1):20-1.
75. Venken K, Hellings N, Thewissen M, Somers V, Hensen K, Rummens JL, et al. Compromised CD4+ CD25(high) regulatory T-cell function in patients with relapsing-remitting multiple sclerosis is correlated with a reduced frequency of FOXP3-positive cells and reduced FOXP3 expression at the single-cell level. Immunology. 2008;123(1):79-89.
76. Feger U, Luther C, Poeschel S, Melms A, Tolosa E, Wiendl H. Increased frequency of CD4+ CD25+ regulatory T cells in the cerebrospinal fluid but not in the blood of multiple sclerosis patients. Clinical and experimental immunology. 2007;147(3):412-8.
77. Viglietta V, Baecher-Allan C, Weiner HL, Hafler DA. Loss of functional suppression by CD4+CD25+ regulatory T cells in patients with multiple sclerosis. J Exp Med. 2004;199(7):971-9.
78. Olivares-Villagomez D, Wang Y, Lafaille JJ. Regulatory CD4(+) T cells expressing endogenous T cell receptor chains protect myelin basic protein-specific transgenic mice from spontaneous autoimmune encephalomyelitis. The Journal of experimental medicine. 1998;188(10):1883-94.
79. Stephens LA, Malpass KH, Anderton SM. Curing CNS autoimmune disease with myelin-reactive Foxp3+ Treg. European journal of immunology. 2009;39(4):1108-17.
80. Fransson M, Piras E, Burman J, Nilsson B, Essand M, Lu B, et al. CAR/FoxP3-engineered T regulatory cells target the CNS and suppress EAE upon intranasal delivery. Journal of neuroinflammation. 2012;9:112.
81. Korn T, Reddy J, Gao W, Bettelli E, Awasthi A, Petersen TR, et al. Myelin-specific regulatory T cells accumulate in the CNS but fail to control autoimmune inflammation. Nature medicine. 2007;13(4):423-31.
82. O'Connor RA, Malpass KH, Anderton SM. The inflamed central nervous system drives the activation and rapid proliferation of Foxp3+ regulatory T cells. J Immunol. 2007;179(2):958-66.
83. Lowther DE, Chong DL, Ascough S, Ettorre A, Ingram RJ, Boyton RJ, et al. Th1 not Th17 cells drive spontaneous MS-like disease despite a functional regulatory T cell response. Acta neuropathologica. 2013;126(4):501-15.
84. Goverman J. Autoimmune T cell responses in the central nervous system. Nature reviews Immunology. 2009;9(6):393-407.
85. Chastain EM, Duncan DS, Rodgers JM, Miller SD. The role of antigen presenting cells in multiple sclerosis. Biochimica et biophysica acta. 2011;1812(2):265-74.
86. Lang HL, Jacobsen H, Ikemizu S, Andersson C, Harlos K, Madsen L, et al. A functional and structural basis for TCR cross-reactivity in multiple sclerosis. Nat Immunol. 2002;3(10):940-3.

87. Shechter R, London A, Schwartz M. Orchestrated leukocyte recruitment to immune-privileged sites: absolute barriers versus educational gates. Nature reviews Immunology. 2013;13(3):206-18.
88. Schetters STT, Gomez-Nicola D, Garcia-Vallejo JJ, Van Kooyk Y. Neuroinflammation: Microglia and T Cells Get Ready to Tango. Front Immunol. 2017;8:1905.
89. Ellwardt E, Walsh JT, Kipnis J, Zipp F. Understanding the Role of T Cells in CNS Homeostasis. Trends Immunol. 2016;37(2):154-65.
90. de Vos AF, van Meurs M, Brok HP, Boven LA, Hintzen RQ, van der Valk P, et al. Transfer of Central Nervous System Autoantigens and Presentation in Secondary Lymphoid Organs. The Journal of Immunology. 2002;169(10):5415-23.
91. Mundt S, Greter M, Flügel A, Becher B. The CNS Immune Landscape from the Viewpoint of a T Cell. Trends in neurosciences. 2019;42(10):667-79.
92. Waisman A, Johann L. Antigen-presenting cell diversity for T cell reactivation in central nervous system autoimmunity. J Mol Med (Berl). 2018;96(12):1279-92.
93. Engelhardt B, Ransohoff RM. Capture, crawl, cross: the T cell code to breach the blood–brain barriers. Trends in Immunology. 2012;33(12):579-89.
94. Larochelle C, Alvarez JI, Prat A. How do immune cells overcome the blood-brain barrier in multiple sclerosis? FEBS letters. 2011;585(23):3770-80.
95. Engelhardt B. Cluster: barriers of the central nervous system. Acta neuropathologica. 2018;135(3):307-10.
96. Lopes Pinheiro MA, Kooij G, Mizee MR, Kamermans A, Enzmann G, Lyck R, et al. Immune cell trafficking across the barriers of the central nervous system in multiple sclerosis and stroke. Biochimica et biophysica acta. 2016;1862(3):461-71.
97. Rothlein R, Dustin ML, Marlin SD, Springer TA. A human intercellular adhesion molecule (ICAM-1) distinct from LFA-1. J. Immunol. 1986. 137: 1270-1274. J Immunol. 2011;186(9):5034-8.
98. Mori K, Fujita SC, Watanabe Y, Obata K, Hayaishi O. Telencephalon-specific antigen identified by monoclonal antibody. Proceedings of the National Academy of Sciences of the United States of America. 1987;84(11):3921-5.
99. Tian L, Yoshihara Y, Mizuno T, Mori K, Gahmberg CG. The neuronal glycoprotein telencephalin is a cellular ligand for the CD11a/CD18 leukocyte integrin. Journal of immunology (Baltimore, Md : 1950). 1997;158(2):928-36.
100. Tian L, Kilgannon P, Yoshihara Y, Mori K, Gallatin WM, Carpen O, et al. Binding of T lymphocytes to hippocampal neurons through ICAM-5 (telencephalin) and characterization of its interaction with the leukocyte integrin CD11a/CD18. European journal of immunology. 2000;30(3):810-8.
101. Tian L, Stefanidakis M, Ning L, Van Lint P, Nyman-Huttunen H, Libert C, et al. Activation of NMDA receptors promotes dendritic spine development through MMP-mediated ICAM-5 cleavage. The Journal of cell biology. 2007;178(4):687-700.
102. Gahmberg CG, Tian L, Ning L, Nyman-Huttunen H. ICAM-5--a novel two-facetted adhesion molecule in the mammalian brain. Immunology letters. 2008;117(2):131-5.
103. Tian L, Lappalainen J, Autero M, Hänninen S, Rauvala H, Gahmberg CG. Shedded neuronal ICAM-5 suppresses T-cell activation. Blood. 2008;111(7):3615-25.
104. Svoboda K, Yasuda R. Principles of two-photon excitation microscopy and its applications to neuroscience. Neuron. 2006;50(6):823-39.
105. Rocheleau JV, Piston DW. Two-photon excitation microscopy for the study of living cells and tissues. Current protocols in cell biology. 2003;Chapter 4:Unit 4.11.
106. Denk W, Strickler JH, Webb WW. Two-photon laser scanning fluorescence microscopy. Science (New York, NY). 1990;248(4951):73-6.
107. Rubart M. Two-photon microscopy of cells and tissue. Circulation research. 2004;95(12):1154-66.
108. Helmchen F, Imoto K, Sakmann B. Ca2+ buffering and action potential-evoked Ca2+ signaling in dendrites of pyramidal neurons. Biophysical Journal. 1996;70(2):1069-81.

109. Siffrin V, Birkenstock J, Luchtman DW, Gollan R, Baumgart J, Niesner RA, et al. FRET based ratiometric Ca(2+) imaging to investigate immune-mediated neuronal and axonal damage processes in experimental autoimmune encephalomyelitis. J Neurosci Methods. 2015;249:8-15.
110. Trachtenberg JT, Chen BE, Knott GW, Feng G, Sanes JR, Welker E, et al. Long-term in vivo imaging of experience-dependent synaptic plasticity in adult cortex. Nature. 2002;420(6917):788-94.
111. Lichtman JW, Fraser SE. The neuronal naturalist: watching neurons in their native habitat. Nature neuroscience. 2001;4 Suppl:1215-20.
112. Nimmerjahn A, Kirchhoff F, Helmchen F. Resting Microglial Cells Are Highly Dynamic Surveillants of Brain Parenchyma in Vivo. Science (New York, NY). 2005;308(5726):1314-8.
113. Herz J, Paterka M, Niesner RA, Brandt AU, Siffrin V, Leuenberger T, et al. In vivo imaging of lymphocytes in the CNS reveals different behaviour of naïve T cells in health and autoimmunity. Journal of neuroinflammation. 2011;8:131.
114. Ransohoff RM, Kivisäkk P, Kidd G. Three or more routes for leukocyte migration into the central nervous system. Nature reviews Immunology. 2003;3(7):569-81.
115. Siffrin V, Brandt AU, Radbruch H, Herz J, Boldakowa N, Leuenberger T, et al. Differential immune cell dynamics in the CNS cause CD4+ T cell compartmentalization. Brain : a journal of neurology. 2009;132(Pt 5):1247-58.
116. Kawakami N, Flügel A. Knocking at the brain's door: intravital two-photon imaging of autoreactive T cell interactions with CNS structures. Seminars in immunopathology. 2010;32(3):275-87.
117. Mazurier F, Fontanellas A, Salesse S, Taine L, Landriau S, Moreau-Gaudry F, et al. A novel immunodeficient mouse model--RAG2 x common cytokine receptor gamma chain double mutants--requiring exogenous cytokine administration for human hematopoietic stem cell engraftment. J Interferon Cytokine Res. 1999;19(5):533-41.
118. Livak KJ, Schmittgen TD. Analysis of relative gene expression data using real-time quantitative PCR and the 2(-Delta Delta C(T)) Method. Methods (San Diego, Calif). 2001;25(4):402-8.
119. Williams JL, Manivasagam S, Smith BC, Sim J, Vollmer LL, Daniels BP, et al. Astrocyte-T cell crosstalk regulates region-specific neuroinflammation. Glia. 2020:10.1002/glia.23783.
120. Stromnes IM, Cerretti LM, Liggitt D, Harris RA, Goverman JM. Differential regulation of central nervous system autoimmunity by T(H)1 and T(H)17 cells. Nat Med. 2008;14(3):337-42.
121. Kroenke MA, Carlson TJ, Andjelkovic AV, Segal BM. IL-12- and IL-23-modulated T cells induce distinct types of EAE based on histology, CNS chemokine profile, and response to cytokine inhibition. J Exp Med. 2008;205(7):1535-41.
122. Rothhammer V, Heink S, Petermann F, Srivastava R, Claussen MC, Hemmer B, et al. Th17 lymphocytes traffic to the central nervous system independently of alpha4 integrin expression during EAE. J Exp Med. 2011;208(12):2465-76.
123. Nakanishi K, Yoshimoto T, Tsutsui H, Okamura H. Interleukin-18 regulates both Th1 and Th2 responses. Annual review of immunology. 2001;19:423-74.
124. Tian L, Stefanidakis M, Ning L, Van Lint P, Nyman-Huttunen H, Libert C, et al. Activation of NMDA receptors promotes dendritic spine development through MMP-mediated ICAM-5 cleavage. Journal of Cell Biology. 2007;178(4):687-700.
125. Birkner K, Loos J, Gollan R, Steffen F, Wasser B, Ruck T, et al. Neuronal ICAM-5 Plays a Neuroprotective Role in Progressive Neurodegeneration. Frontiers in neurology. 2019;10:205.
126. Constantinescu CS, Farooqi N, O'Brien K, Gran B. Experimental autoimmune encephalomyelitis (EAE) as a model for multiple sclerosis (MS). Br J Pharmacol. 2011;164(4):1079-106.
127. Kroenke MA, Segal BM. IL-23 modulated myelin-specific T cells induce EAE via an IFNγ driven, IL-17 independent pathway. Brain Behav Immun. 2011;25(5):932-7.
128. Kroenke MA, Chensue SW, Segal BM. EAE mediated by a non-IFN-γ/non-IL-17 pathway. European journal of immunology. 2010;40(8):2340-8.
129. Gran B, Zhang GX, Yu S, Li J, Chen XH, Ventura ES, et al. IL-12p35-deficient mice are susceptible to experimental autoimmune encephalomyelitis: evidence for redundancy in the IL-12

system in the induction of central nervous system autoimmune demyelination. J Immunol. 2002;169(12):7104-10.
130. Kasper LH, Everitt D, Leist TP, Ryan KA, Mascelli MA, Johnson K, et al. A phase I trial of an interleukin-12/23 monoclonal antibody in relapsing multiple sclerosis. Curr Med Res Opin. 2006;22(9):1671-8.
131. Segal BM, Constantinescu CS, Raychaudhuri A, Kim L, Fidelus-Gort R, Kasper LH. Repeated subcutaneous injections of IL12/23 p40 neutralising antibody, ustekinumab, in patients with relapsing-remitting multiple sclerosis: a phase II, double-blind, placebo-controlled, randomised, dose-ranging study. The Lancet Neurology. 2008;7(9):796-804.
132. Ulzheimer JC, Meuth SG, Bittner S, Kleinschnitz C, Kieseier BC, Wiendl H. Therapeutic approaches to multiple sclerosis: an update on failed, interrupted, or inconclusive trials of immunomodulatory treatment strategies. BioDrugs. 2010;24(4):249-74.
133. Martin R. Neutralisation of IL12 p40 or IL23 p40 does not block inflammation in multiple sclerosis. The Lancet Neurology. 2008;7(9):765-6.
134. Huang WX, Huang P, Hillert J. Increased expression of caspase-1 and interleukin-18 in peripheral blood mononuclear cells in patients with multiple sclerosis. Multiple sclerosis (Houndmills, Basingstoke, England). 2004;10(5):482-7.
135. Wildbaum G, Youssef S, Grabie N, Karin N. Neutralizing antibodies to IFN-gamma-inducing factor prevent experimental autoimmune encephalomyelitis. J Immunol. 1998;161(11):6368-74.
136. Jander S, Stoll G. Differential induction of interleukin-12, interleukin-18, and interleukin-1β converting enzyme mRNA in experimental autoimmune encephalomyelitis of the Lewis rat. Journal of Neuroimmunology. 1998;91(1):93-9.
137. Rex DAB, Agarwal N, Prasad TSK, Kandasamy RK, Subbannayya Y, Pinto SM. A comprehensive pathway map of IL-18-mediated signalling. J Cell Commun Signal. 2020;14(2):257-66.
138. Yoshimoto T, Takeda K, Tanaka T, Ohkusu K, Kashiwamura S, Okamura H, et al. IL-12 up-regulates IL-18 receptor expression on T cells, Th1 cells, and B cells: synergism with IL-18 for IFN-gamma production. J Immunol. 1998;161(7):3400-7.
139. Cosmi L, Cimaz R, Maggi L, Santarlasci V, Capone M, Borriello F, et al. Evidence of the transient nature of the Th17 phenotype of CD4+CD161+ T cells in the synovial fluid of patients with juvenile idiopathic arthritis. Arthritis & Rheumatism. 2011;63(8):2504-15.
140. Basdeo SA, Cluxton D, Sulaimani J, Moran B, Canavan M, Orr C, et al. Ex-Th17 (Nonclassical Th1) Cells Are Functionally Distinct from Classical Th1 and Th17 Cells and Are Not Constrained by Regulatory T Cells. The Journal of Immunology. 2017;198(6):2249-59.
141. Hirota K, Duarte JH, Veldhoen M, Hornsby E, Li Y, Cua DJ, et al. Fate mapping of IL-17-producing T cells in inflammatory responses. Nature Immunology. 2011;12(3):255-63.
142. Tian L, Lappalainen J, Autero M, Hanninen S, Rauvala H, Gahmberg CG. Shedded neuronal ICAM-5 suppresses T-cell activation. Blood. 2008;111(7):3615-25.
143. Brosnan CF, Cannella B, Battistini L, Raine CS. Cytokine localization in multiple sclerosis lesions: correlation with adhesion molecule expression and reactive nitrogen species. Neurology. 1995;45(6 Suppl 6):S16-21.
144. Paetau S, Rolova T, Ning L, Gahmberg CG. Neuronal ICAM-5 Inhibits Microglia Adhesion and Phagocytosis and Promotes an Anti-inflammatory Response in LPS Stimulated Microglia. Front Mol Neurosci. 2017;10:431.
145. Lindsberg PJ, Launes J, Tian L, Valimaa H, Subramanian V, Siren J, et al. Release of soluble ICAM-5, a neuronal adhesion molecule, in acute encephalitis. Neurology. 2002;58(3):446-51.
146. Di Battista AP, Buonora JE, Rhind SG, Hutchison MG, Baker AJ, Rizoli SB, et al. Blood Biomarkers in Moderate-To-Severe Traumatic Brain Injury: Potential Utility of a Multi-Marker Approach in Characterizing Outcome. Front Neurol. 2015;6:110.